Recent Advances in the Synthesis of Conjugated Polymers for Supercapacitors

Citation for the original published paper (version of record):
Wolkeba, Z., Xia, Z., Yang, G. et al (2024). Recent Advances in the Synthesis of Conjugated Polymers for Supercapacitors. Advanced Materials Technologies, 9(9).
http://dx.doi.org/10.1002/admt.202300167

ADVANCED MATERIALS TECHNOLOGIES
www.advmattechnol.de

Recent Advances in the Synthesis of Conjugated Polymers for Supercapacitors

*Zewdneh Genene, Zhenyuan Xia, Guijun Yang, Wendimagegn Mammo, and Ergang Wang**

Conjugated polymers have attracted growing attention for versatile applications in energy storage due to their potential benefits including low-cost processing, molecular tunability, environmental benignity, and high mechanical flexibility. In particular, polymer-based organic electrode materials have shown significant progress in supercapacitor (SC) applications with superior electrochemical behaviors. The performances of SCs are closely related to the intrinsic characteristics of different polymers in the nanoscale and the morphological features of the polymer-based electrode materials obtained by different fabrication techniques in the macroscale. This review summarizes the design and synthesis of both *p*-type and *n*-type conjugated polymers, highlighting the pros and cons of three synthesis techniques: electrochemical polymerization, chemical polymerization, and in situ polymerization. The performances of conjugated polymers in SCs, their cycling stabilities, and structure-performance relationships are discussed. Moreover, the existing challenges and future directions of polymer-based SCs are considered with respect to energy density, stability, and large-scale production to promote commercialization.

1. Introduction

The ever-growing energy demand and depletion of fossil fuel reserves, together with impending environmental pollution, have prompted the development of sustainable and renewable alternative power sources. Recent years have witnessed significant strides in the advancement of alternative energy generation technologies based on renewable energy sources such as photovoltaic technology and wind power. Since the sun doesn't shine consistently and the wind doesn't blow all the time, the electrical energy derived from renewable energy sources must be stored efficiently for continuous power supply. Furthermore, the electrification of the transport sector and the burgeoning demand for long-life wireless internet of things (IoT) appliances and smart devices need more efficient energy storage technologies to ensure uninterrupted and continuous power supply.[1–3]

Electrochemical energy storage devices such as batteries and supercapacitors (SCs) play a significant role in powering electrical and electronic devices with high performance at affordable prices. Owing to high energy storage ability (up to 250 Wh kg^{-1}), lithium-ion batteries (LIBs) have been utilized in portable electronic devices including smartphones, tablets, laptop computers, wearable devices, and vehicles.[4–6] However, the low power density (≈10^2 W kg^{-1}), short lifetime (<4000 cycles), and slow kinetics of LIBs, limit their application in emerging electrical and electronic devices.[7,8] On the other hand, SCs present high power density (≈10^4 W kg^{-1}), rapid charge/discharge capability, and long-term cycling stability (>10 000 cycles) that make them promising and ideal complements to LIBs.[9] Conventional SCs usually consist of positive/negative electrode materials, current collectors, electrolytes, and separators that prevent physical contact and short-circuiting of the electrodes but permit the permeation of ions. Currently, SCs are being employed in different devices such as emergency power, electric vehicles, medical equipment, and consumer electronics.[10] Unlike LIBs, conventional SCs deliver low energy density (up to 10 Wh kg^{-1}) which restricts their commercial application. Thus, great efforts have been devoted to enhancing the energy density of SCs while keeping their high power density performance. To realize high-energy-density SCs, it is crucial to develop novel electrode materials with low-cost, earth-abundant elements, and sustainable processing features.[11]

SCs can be classified into electrical double-layer capacitors (EDLCs), pseudocapacitors, and hybrid-type capacitors

Z. Genene, G. Yang, E. Wang
Department of Chemistry and Chemical Engineering
Chalmers University of Technology
Göteborg SE-412 96, Sweden
E-mail: ergang@chalmers.se
Z. Xia
Department of Industrial and Materials Science
Chalmers University of Technology
Gothenburg SE-412 96, Sweden
W. Mammo
Department of Chemistry
Addis Ababa University
Addis Ababa 33658, Ethiopia

The ORCID identification number(s) for the author(s) of this article can be found under https://doi.org/10.1002/admt.202300167

DOI: 10.1002/admt.202300167

with battery-like behaviors, based on their charge storage mechanisms.[12,13] In EDLCs, the charge is stored through electrostatic charge accumulation at the electrode/electrolyte interface.[2,14] On the other hand, in pseudocapacitors, charges are stored by a fast and reversible capacitive Faradaic process at or near the electrode surface with ion diffusion to balance the oxidized and reduced states.[14] Similarly, battery-type capacitors also involve Faradaic reactions inside the electrode materials, but the electrode reaction is a Nernstian charge/discharge diffusion-controlled process (or non-capacitive Faradaic process) with crystallographic phase changes.[15] Both pseudocapacitors and battery-type capacitors possess superior specific capacitance and energy density, which could be 10–100 times higher than that of EDLCs.[16]

To facilitate an efficient charge storage mechanism, various materials can be employed. Carbon materials, including activated carbon,[17] carbon nanotubes,[18] and graphene[19] show promise as SC electrodes due to their unique properties such as high surface area, excellent electrical conductivity, extraordinary elasticity, and ultra-lightweight. For example, activated carbons, the most widely used EDLC electrode materials, deliver high power density but limited energy density (<10 Wh kg^{-1}).[20]

Redox-active materials, characterized by functional groups capable of undergoing reversible reduction or oxidation processes, such as metal oxides[21,22] and conjugated polymers[23,24] have been used as active materials for pseudocapacitive and battery-type SCs. In particular, polymer-based materials, which usually possess both capacitive and battery-type behaviors, have sparked much keen interest due to several advantages of polymers over metal oxides including high electronic conductivity, lower production cost, high conductivity (>10^3 S cm^{-1}) wide potential window, light weight, good environmental stability and fast switching responses during doping/dedoping processes.[25–27] Furthermore, solution processability mechanical robustness, and flexibility of conjugated polymers enable large-area, portable, stretchable, or flexible SC fabrication.[28,29] Conjugated polymers can be classified based on the number and type of the building blocks as homopolymers consisting of one type of monomer, donor-acceptor (D-A) copolymers consisting of two types of monomers (donor and acceptor units), and terpolymers with three types of monomers.[30,31] As compared to homopolymers, the optical and redox properties of D-A copolymers and terpolymers can be easily tuned by combining different electron-rich and electron-poor units as well as by incorporating different side chains. Depending on whether they are easily oxidized or reduced, conjugated polymers are further classified as p-type (p-doped) or n-type (n-doped), respectively. The p-type polymers stabilize the positive charge in the highest occupied molecular orbital (HOMO) levels while the n-type polymers stabilize the negative charge in the lowest unoccupied molecular orbital (LUMO) levels.[32,33]

Polymer-based capacitors could store charge by a reversible electrochemical doping mechanism which is determined by a quasi-rectangular cyclic voltammogram that may have a set of reversible redox peaks due to the battery-type reaction. This mechanism involves either the reduction of the polymer with the simultaneous insertion of a cation from the electrolyte (n-doping) or the oxidation of the polymer with simultaneous anion insertion (p-doping) during the charge/discharge process. This results in delocalized charge carriers along the polymer chains.[2,24,34]

Significant efforts have been dedicated to designing and synthesizing novel redox-active polymers to enhance the electrochemical performances of conjugated polymer-based SCs. Polymerization methods including electrochemical polymerization, solid-state polymerization, vapor-phase polymerization, solution-processable polymerization, and water-based nano-emulsion polymerization were utilized to synthesize the polymers.[29] Several reviews that cover the progress of polymer-based SCs have been published.[27,29,35–38] Nonetheless, most of them focus on the applications of homopolymers such as polyaniline, polypyrrole, polythiophene, and poly(3,4-ethylenedioxythiophene) and their composites and only a few of the reviews give due emphasis to the design and synthesis of both p-type and n-type polymers for SCs using different polymerization methods. Moreover, there is no systematic review of the recent progress in the synthesis and application of all kinds of conjugated polymers for SC applications. In this review, we highlight the recent developments in high-performance p-type and n-type polymers for SCs, including homopolymers, copolymers, and terpolymers, as well as the synthetic approaches used to prepare them, such as electropolymerization, chemical polymerization, and in situ polymerization. We also summarize the structure-property relationships of these conjugated polymers and their hybrid composites made of 2D materials (such as graphene and MXene) or biopolymers in SCs and strategies to achieve high capacitance, energy density, and cycling stability. Finally, the current challenges facing polymer-based SCs and future outlooks for this promising capacitor material are discussed.

2. State of the Art Supercapacitors Based on Polymers

Over the years, various p-type and n-type polymers have been studied to enhance the capacitance and energy density of SCs. Specific capacitance (C_s) values higher than 1600 F g^{-1} in half cells and 1335 F g^{-1} in symmetric SCs were recorded for p-type polymers.[39–41] On the other hand, n-type polymers achieved C_s close to 700 F g^{-1} in half-cell SCs.[42] The devices showed fast charge/discharge rates and lifetimes of over 5 0000 cycles, which make the conjugated polymer-based SCs very promising for commercialization.

2.1. Device Structures and Performance Parameters of Polymer-Based Capacitors

EDLCs, pseudocapacitors, and battery-type capacitors have similar device structures but differ in their storage mechanism and electrode types. All types of SCs contain two electrodes separated by an insulator (separator) immersed in an electrolyte.[43] **Figure 1** shows schematic illustrations of the cyclic voltammograms (CVs) of EDLC, pseudocapacitive, and battery-type materials. EDLC materials display CVs that are rectangular. On the other hand, the CVs of pseudocapacitive materials exhibit broad redox peaks (quasi-rectangular shapes), while battery-type materials show a couple of well-defined redox peaks due to the crystallographic phase transformation.[2]

According to the intrinsic physicochemical properties of conjugated polymers, polymer-based capacitors with both pseudocapacitive and battery-like performance can be further classified as

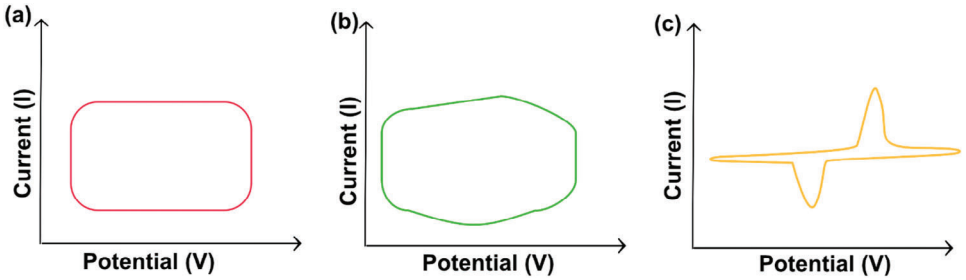

Figure 1. Schematic illustrations of the CVs of a) EDLC, b) pseudocapacitive, and c) battery-type materials.

type I, type II, type III, and type IV devices.[24,44] **Figure 2** depicts schematic cyclic voltammograms of the four types of devices. Type I devices (symmetric SCs) consist of the same p-dopable (p-type) polymers for both anode and cathode materials (Figure 2a). Such devices have limitations including the fact that only half of the stored energy can be released, and the cell voltage is restricted by the potential window to one of the p-dopable polymers (usually in the range of 0.5–0.75 V in aqueous electrolytes), thus delivering low energy density. Type II devices (asymmetric SCs) utilize two different p-type polymers having complementary potential windows and result in a transfer of more than half of the stored charge, higher cell voltage, and energy density than type I devices (Figure 2b).[45] Type III devices (symmetric SCs) employ ambipolar polymers that are p- and n-dopable for both electrodes (Figure 2c).[46] The p-doped forms are used as the positive electrodes and the n-doped forms as the negative electrodes. The cell voltages of type III devices have the potential to be higher than what can be attained in type I and II devices.

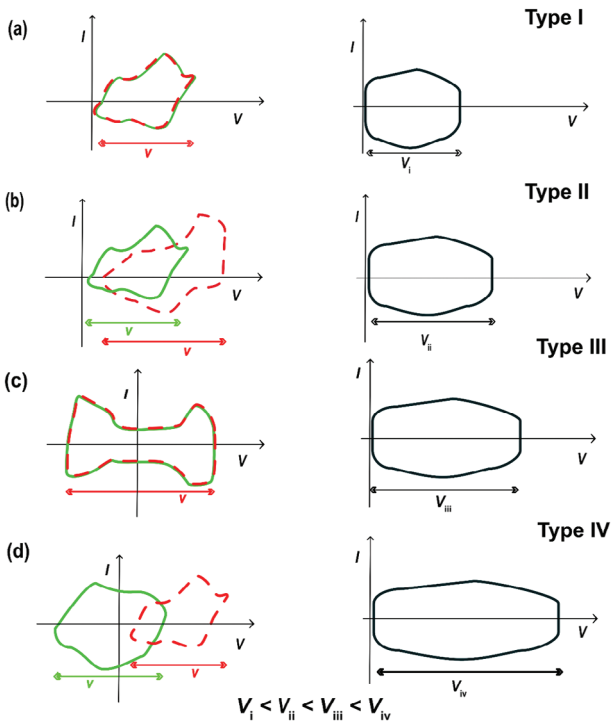

Figure 2. Schematic cyclic voltammograms of polymers from half cell (left) and full cell device (right) with green solid voltammograms as a negative electrode and red dashed voltammograms as a positive electrode for a) type I devices: symmetric SCs with the same p-type polymer, b) type II devices: asymmetric SCs with two different p-type polymers, c) type III devices: symmetric SCs with ambipolar polymers, and d) type IV devices: asymmetric SCs with dissimilar polymers.

Type IV devices (asymmetric SCs) use two dissimilar polymers for the positive and negative electrodes (Figure 2d). In these types of devices, p-type polymers can be used as positive electrodes and n-type polymers as negative electrodes, each with different potential windows, where the overlapped/non-overlapped potential windows of the electrodes are added together leading to high cell voltages.[47] Hence, among the four types of pseudocapacitors, asymmetric devices deliver the highest energy density.[48] However, asymmetric pseudocapacitors have not been explored very well, as compared to symmetric devices, due to the dearth of stable n-type polymers.

To evaluate the performance of a supercapacitor device, the three figures of merit, i.e., energy density, power density, and cycling stability, are largely assessed. The C_s of a material can be examined by using CV, galvanostatic charge-discharge (GCD), and electrochemical impedance spectroscopy. The calculation based on GCD can use the equation $C_s = \frac{I\Delta t}{x\Delta V}$, where I, Δt, and ΔV are the current, discharge time, and potential window, respectively, and x can be the area, mass, or volume of the electrodes to calculate the corresponding areal, gravimetric, and volumetric specific capacitances, respectively.[49]

The energy density (E_D, Wh kg^{-1}) of a SC can be determined from the C_s and cell voltage (V) of the device based on $E_D = \frac{1}{2} C_s V^2$. Thus, enhancing either one or both the capacitance and operational potential window will increase the energy density of the device. The C_s of SCs based on polymers depend on the physicochemical properties of the polymers including redox activity, conductivity, doping level, charge mobility, crystal structure, morphology, surface area, pore size, and ion diffusion efficiency. These properties of the conjugated polymers have been improved by tuning the chemical structures of the polymers and optimizing the electrode preparation. Furthermore, SCs can also achieve high capacitance and wide potential windows by selecting suitable electrolytes and device types. Pseudocapacitive and battery-type capacitors are also designed to deliver high power density (P_D, W kg^{-1}), which is estimated based on $P_D = \frac{E_D}{\Delta t}$, where Δt is the discharge time. Since there is inconsistency in the calculation of E_D and P_D, it is difficult to make direct comparisons. Thus, in this review, we have made comparisons between the performances of the materials largely based on the mass C_s. For a more detailed characterization of

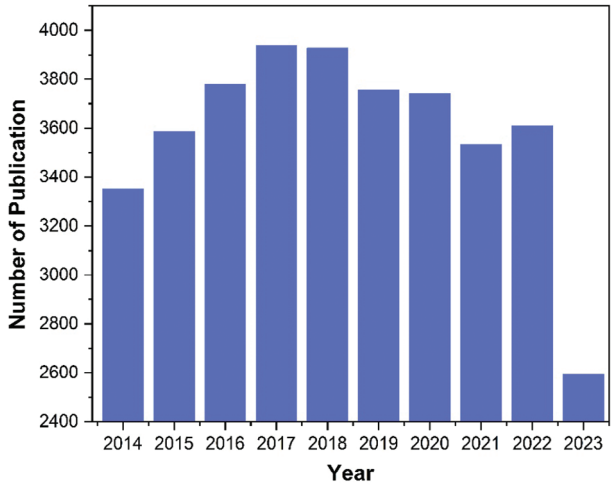

Figure 3. Number of publications on the topic "conjugated polymers" during the past years, according to Web of Science.

the figure of merits, we refer readers to review articles that focus on the performance evaluation of SCs.[49,50]

3. Synthesis of Conjugated Polymers for Supercapacitors

3.1. History of Conjugated Polymers for Supercapacitors

The application of conjugated polymers in organic electronic devices has been extensively studied following the pioneering work by Shirakawa, MacDiarmid, and Heeger in 1997.[51] A wide array of polymers like homopolymers, D-A copolymers, and terpolymers have been synthesized which gave high performances in organic solar cells,[30,52,53] organic light-emitting diodes,[54] organic field-effect transistors,[55] light-emitting electrochemical cells[56] and photodetectors.[57] The quantity of publications on conjugated polymers has consistently remained high over the past years, underscoring significant interest in their development, as shown in **Figure 3**. Polyacetylene is the first polymer that was used for energy storage due to its n-doping and p-doping capabilities.[58] However, the development of polyacetylene-based batteries was jeopardized because of innate instability and processing difficulties.[59] The abilities of other polymers to store charges and their potential applications for SCs have been extensively investigated.[60] The most common polymers utilized for SCs include polyaniline (PANI), polypyrrole (PPy), polythiophene (PTh), and poly(3,4-ethylenedioxythiophene) (PEDOT) (**Figure 4**).

The synthesis methods employed for the preparation of conjugated polymers profoundly influence their physical and chemical properties, including conductivity, morphology, and electrochemical stability. These crucial properties, in turn, have a substantial impact on the ultimate performances of SCs that utilize polymers as electrode materials. Hence, the careful selection of an appropriate synthesis method plays a pivotal role in attaining the desired characteristics necessary for high-performance SCs.[59] Polymers utilized in SCs have been prepared using various approaches, including electrochemical polymerization (electropolymerization), in situ polymerization, and chemical polymerization techniques. In this section, the synthesis of polymers by these three polymerization methods and their electrochemical performances will be discussed.

3.2. Electrochemical Polymerization

Electrochemical polymerization (EP) is the most widely employed method for preparing conjugated polymers used in energy storage and various electronic devices.[61] In general, electropolymerization involves three steps: i) oxidation of the monomer into a cation-radical, ii) coupling of two cation-radicals, and, iii) re-aromatization via deprotonation. This provides an oligomer that further forms a film by deposition, accompanied by nucleation and growth processes to form longer polymer chains.[62]

EP is a simple and cost-effective technique that offers several advantages for energy storage applications. The advantages include: i) direct deposition of polymers onto the charge collector surface, enabling control over the rate of polymerization and doping level without the need for a binder, which could otherwise reduce electrode conductivity; ii) solvent resistance of the resulting polymeric films; and iii) highly porous polymer electrodes with a large surface area, promoting efficient ion diffusion in high-performance SCs.

3.2.1. Homopolymers Synthesized by EP

Conventional polymers, primarily homopolymers, have been extensively employed as electrode materials for electrochemical energy storage owing to their high electrical conductivity, significant pseudocapacitance, and cost-effectiveness. Figure 4 illustrates the most widely used homopolymers synthesized via EP. The structures of other polymers prepared by EP for energy storage applications are depicted in **Figures 5** and **6**.

PANI is one of the most widely used polymers for SCs. It can be synthesized through the EP of aniline monomer and has advantages such as unusual reversible doping/dedoping chemistry, environmental stability, and high specific pseudocapacitance associated with multiple redox states.[23] For example, vertically aligned PANI nanowires were deposited on an Au electrode by EP of aniline.[63] Application of this electrode in a SC using 1M $HClO_4$ as an electrolyte afforded a high C_s of 950 F g^{-1} at 1 A g^{-1}.

Another polymer that has been intensively studied as an electrode material for SCs is polypyrrole (PPy), which possesses high thermal stability, a fast charge-discharge mechanism a relatively high theoretical specific capacity of 75 mAh g^{-1}, and a specific energy density of up to 390 Wh kg^{-1}.[64] Dubal et al.[65] used the EP method to develop various nanostructures of PPy on stainless steel for SC applications. The PPy nanosheets showed the highest C_s of 586 F g^{-1} at a scan rate of 2 mV s^{-1} as compared to other nanostructures. Generally, PANI and PPy showed lower pseudocapacitive performances as compared to the theoretically expected values and exhibited poor stability that limited their application in SCs.[66] Thus, several strategies, including the synthesis of binary and ternary composites with carbon-based materials and metal oxides and optimizing the morphology of the electrode, have been used to improve the capacitance and

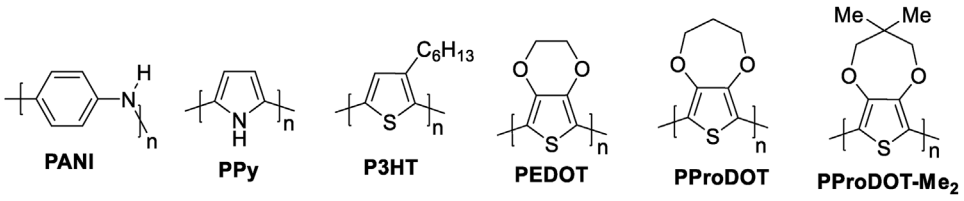

Figure 4. Chemical structures of common conjugated homopolymers.

cycling stability (will be discussed in the next section).[25,67] Generally, composites using carbon-based materials have several advantages including enhanced conductivity, surface area, mechanical strength, and flexibility, resulting in higher capacitance and cyclic stability. However, it also has some disadvantages such as the increase in cost, challenges associated with synthesis, agglomeration formation, and limited improvement in some parameters.

Polythiophene (PTh) and its derivatives have also been synthesized by EP for SC applications. Li et al.[68] developed PTh infiltrated into TiO_2 nanotubes (TNTs) by the controlled EP of thiophene on TNTs. The PTh/TiO_2 exhibited a C_s of 632 F g^{-1} at 2 A g^{-1} with an E_D of 237 Wh kg^{-1} at P_D of 2100 W kg^{-1} and retention of 89% of the capacitance after 1100 cycles while PTh retained 62% of the capacitance after 1100 cycles. The higher cycling stability of PTh/TiO_2 than the PTh electrode is as-

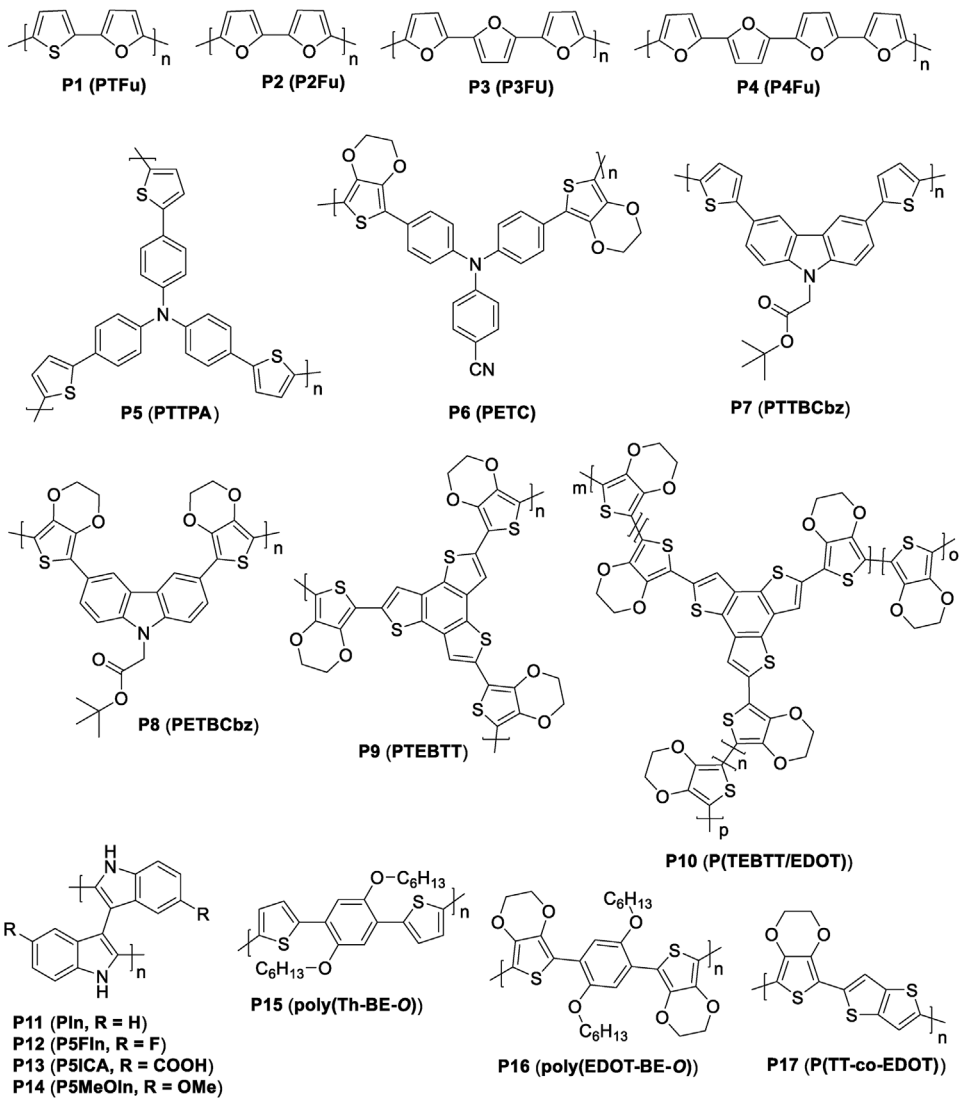

Figure 5. Chemical structures of other conjugated homopolymers (p-type) synthesized by EP.

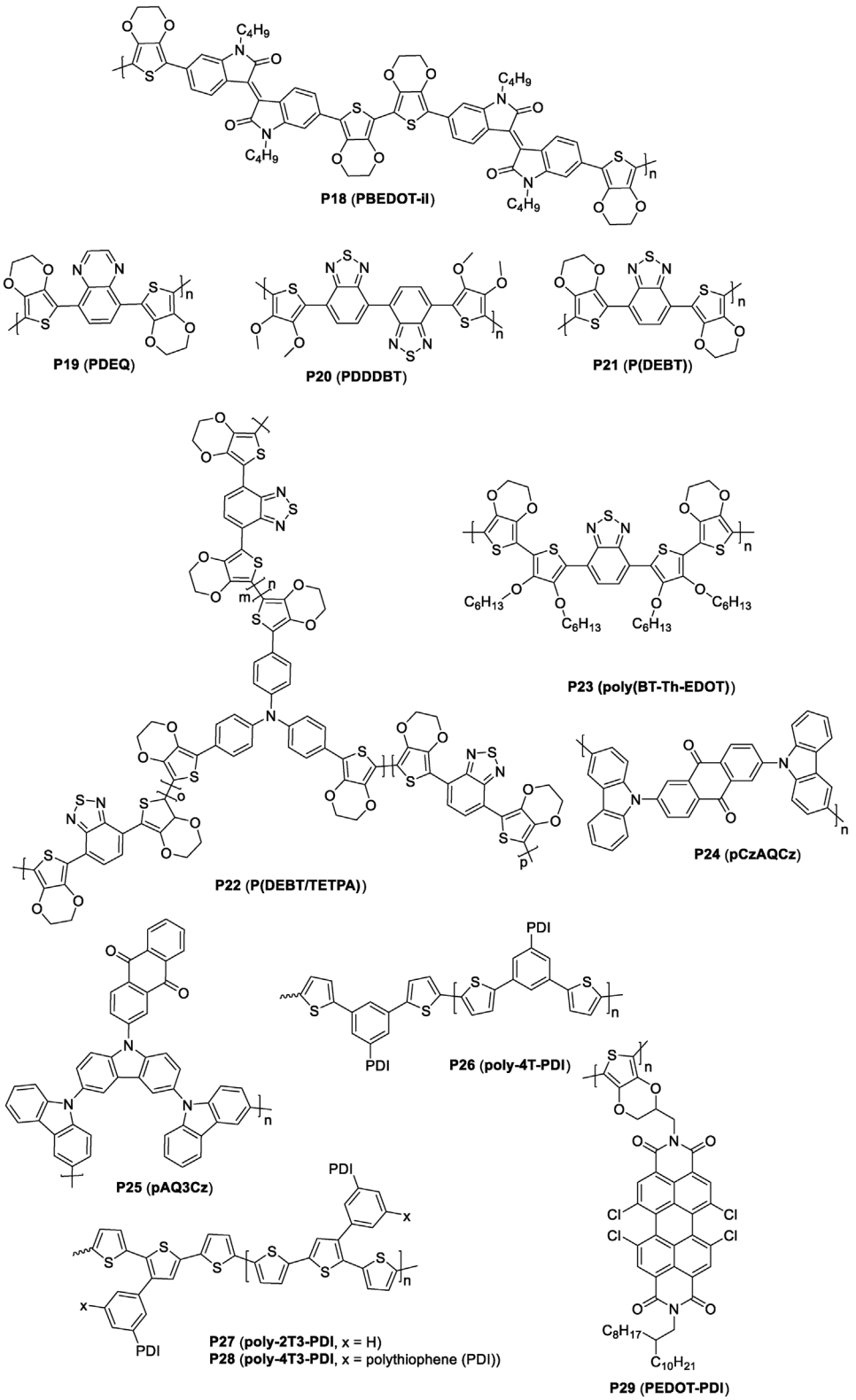

Figure 6. Chemical structures of D-A polymers prepared by the EP method.

cribed to the high mechanical stability of TNTs, which minimizes the swelling of PTh during charging/discharging processes. PEDOT, as one of the polythiophene derivatives, has emerged as a promising pseudocapacitor material due to its high environmental and electrochemical stability over a relatively wide potential window (close to 2.0 V) and thus, it can be used as both positive electrode (p-type) and negative electrode (n-type). Additionally, owing to its high stability in the oxidized state, PEDOT can be used as an electrode in symmetric and asymmetric SCs with both aqueous and organic electrolytes.[69,70] PEDOT made by EP of 3,4-ethylenedioxythiophene (EDOT) on graphite sheet showed a C_s of 126.5 F g^{-1} in type I (symmetrical) SC.[71] Owing to the higher molecular mass of the monomer, the theoretical C_s of PEDOT (210 F g^{-1}) are lower than those of PANI (750 F g^{-1}) and PPy (620 F g^{-1}).[60] However, PEDOT shows higher capacitance when blended with other materials and used as an n-type electrode in conjugated polymer-based asymmetric SCs.[45]

Xu et al.[72] prepared poly(2-(thiophen-2-yl)furan) (**P1**) by EP of 2-(thiophen-2-yl)furan monomer and achieved a C_s of 392.0 F g^{-1} at 5 A g^{-1} in half cell. However, the polymer showed low stability with 67.0% capacitance retention after 500 cycles. Very recently, Jiang et al.[73] developed a series of flexible free-standing polyfuran **P2**-**P4** films by EP of 2,2′-bifuran (2Fu), 2,2′:5′,2″-terfuran (3Fu), and 2,2′:5′,2″:5″,2‴-quaterfuran (4Fu), respectively, and systematically investigated their performances. All the polymers featured pseudocapacitive behaviors. **P4** showed a high C_s of 241.6 F g^{-1} at 1.0 A g^{-1} while **P2** and **P3** exhibited C_s of 117.7 F g^{-1} and 219.5 F g^{-1} at 1 A g^{-1}, respectively (half-cell). The polymers also showed color changes during charging and discharging. Especially, the **P4** film revealed a reversible color change from red to green and then to black and achieved high coloration efficiency. However, the cyclic stabilities of the furan-containing polymers were very low (67.0% retention after 500 cycles for **P1** and 70% retention after 200 cycles for **P4**) as compared with other polymers.

A dendritic polymer poly(tris(4-(thiophen-2-yl)phenyl)amine) (**P5**, Figure 5) is another polythiophene derivative that was synthesized by EP from tris(4-(thiophen-2-yl)phenyl)amine for SCs.[74] This polymer film showed a combination of pseudocapacitive and battery-type behaviors with a high C_s of 990 F g^{-1} for a half cell in an organic electrolyte at scan rates as high as 50 mV s^{-1}, with E_D and P_D over 25 Wh kg^{-1} and 6 kW kg^{-1} at 4 mA cm^{-2}, respectively. Very recently, Chao et al.[75] designed and prepared a twisted polymer **P6** containing dual-redox centers (EDOT and triphenylamine with electron-withdrawing cyano group) by EP. The cyano group lowered the LUMO level of the polymer and improved its redox potential. The polymer showed efficient charge transport properties due to the twisted alignment of the polymer chain. Thus, **P6** attained a maximum areal capacitance of 41.1 mF cm^{-2} (82.2 F g^{-1} or 164.4 F cm^{-3}) at 0.1 mA cm^{-2} in a half cell. Moreover, flexible asymmetric electrochromic SCs containing **P6** as an anode and vanadium pentoxide as cathode with gel electrolyte achieved a high optical contrast of 67%, a wide cell voltage of 2 V, an areal capacitance of 32.9 mF cm^{-2} with an E_D of 18.2 μWh cm^{-2}, 96% optical modulation and 86% capacitance retention after 7000 cycles. The CV and GCD curves of the devices clearly showed pseudocapacitive behavior.

The EP method has also been employed to develop polymer electrode materials with better cycling stability and mechanical flexibility. In this regard, Yiğit and Güllü[76] synthesized **P7** and **P8**, by electropolymerization of carbazole monomers with thiophene and EDOT, respectively, to investigate their performances and cycling stabilities in SCs. During charging/discharging, polarons are formed and energy is stored on the surfaces of the polymers via Faradaic redox reactions based on the proposed mechanism in **Scheme 1**. The symmetric (type I), flexible, solid-state pseudocapacitor devices made from **P8** gave higher C_s of 640 F g^{-1} with E_D of 1280 $^{-1}$ and P_D of 36 kWh kg^{-1}, than **P7**-based devices (C_s = 554 F g^{-1} with an E_D of 1108 Wh kg^{-1} and P_D of 32.7 kWh kg^{-1}), due to more porous two-dimensional surface morphology of **P8**. In addition, the **P8**-based devices showed better mechanical flexibility and cycling stability with capacitance retention of over 90% after 10000 cycles. Among the above homopolymers, PANI and **P8** attained high C_s in a 3-electrode system (half-cell) and type I SCs, respectively.

In addition to homopolymers, EP has also been used to prepare copolymers with highly porous networks. Beaujuge et al.[77] developed copolymer **P10** from tris(ethylenedioxythiophene)benzo[1,2-*b*:3,4-*b*′:5,6-*b*″]trithiophene (TEBTT) and EDOT. The polymer exhibited pseudocapacitive properties with high areal capacitance (as high as 443.8 mF cm^{-2}) due to highly porous hierarchical morphology as compared to the homopolymers **P9** (271.1 mF cm^{-2}) and PEDOT (12.1 mF cm^{-2}) synthesized by the same EP method.

In recent years, smart energy storage devices with multi-functions have attracted the interest of the research community.[78] Conjugated polymers deposited on transparent current collectors can visibly change their colors during redox reactions under external voltage (electrochromism). Hence, the so-called electrochromic SCs have been developed by using electrode materials such as metal oxides[79] and polymers[80–82] that can change their colors during doping/dedoping process. The level of stored energy (charge/discharge state) in these devices can be effortlessly visualized by the color changes. The EP method plays an important role in the preparation of electrode materials for electrochromic SCs.

Polyindoles have received attention for applications in energy storage and electrochromic devices due to their high electrical conductivity, electrochromic characteristics, and thermal stability.[83–85] Recently, Duan et al.[86] synthesized four polyindoles by EP (**Scheme 2**) and investigated their energy storage capacity. Galvanostatic charge/discharge experiments in 1.0 M H_2SO_4 revealed that poly(5-fluoroindole) (**P14**) had a high C_s of 416 F g^{-1} at 10 A g^{-1} with a potential window of 1.25 V and good cycling stability of 83% after 5000 cycles. Under the same conditions, the C_s of polyindole (**P11**), poly(5-methoxyindole) (**P12**), and poly(indole-5-carboxylic acid) (**P13**) were found to be 103, 114, and 286 F g^{-1}, with cyclic stabilities of 68%, 70%, and 70%, respectively. The CV and GCD curves of **P12** and **P13** indicate that both polymers had predominantly battery-type behaviors. It was argued that the fluorine atom in **P14** lowered the LUMO level and improved the morphology by forming hydrogen bonds between F and N-H thereby improving the electrochemical stability and capacitance of **P14**. Nie et al.[87] further enhanced the charge

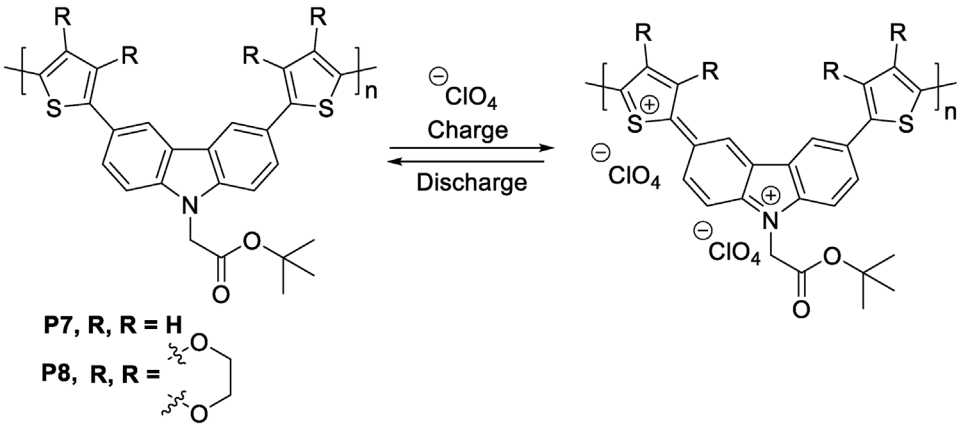

Scheme 1. Faradaic redox mechanisms of **P7** and **P8** (adapted from Ref. [76]).

storage capacity and electrochromic properties of **P13** by EP of 5-indolecarboxylic acid on the surface of WO_3 to form a **P13**/WO_3 nanocomposite which showed a higher C_s of 30.2 mF cm^{-2} (half-cell) than **P13** (14.7 mF cm^{-2}). Furthermore, asymmetric (type IV) electrochromic SC made by using **P13**/WO_3 nanocomposite as a positive electrode and PEDOT as a negative electrode showed a C_s of 10.11 mF cm^{-2} with a coloration efficiency of 608 cm^2 C^{-1}.

The charge/discharge process and electrochromic properties of polymers are related to their doping states (neutral state, polaron, and bipolaron) which depend on the backbone of the polymer and pendant side-chain structure.[88] Duan et al.[89] prepared two electrochromic polymers, **P15** and **P16** based on thiophene or EDOT as a donor unit and bis(hexyloxy)-substituted benzene as a spacer by the EP method. Both polymers demonstrated multiple separate redox couples due to the introduction of hexyloxy side-chains, which is a typical mixed pseudocapacitive and battery-like capacitor property. As a result, the polymers showed a wide voltage range and three different colors in the polaron and bipolaron states. **P16** delivered relatively higher C_s of 97 F g^{-1} than **P15** (64 F g^{-1}) at a current density of 1.0 A g^{-1} due to the better morphology and higher charge transport ability of **P16**. A flexible free-standing copolymer **P17** film, synthesized by electrochemical copolymerization of thieno[3,2-*b*]thiophene with EDOT, was reported very recently.[90] **P17** showed good flexibility, conductivity, and mechanical stability under long-term deformation, color conversion with optical contrast of 50.2% during the charging/discharging process, and attained a high C_s of 193 F g^{-1} at 4 A g^{-1} in a half cell as compared to polythieno[3,2-*b*]thiophene (73 F g^{-1}) and PEDOT (152 F g^{-1}).

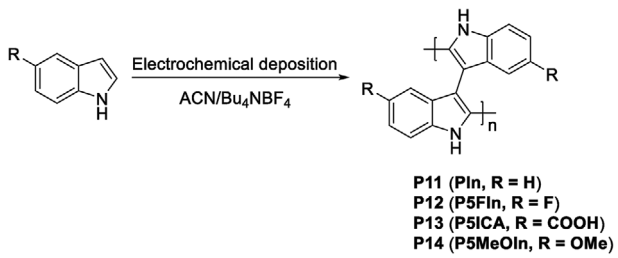

Scheme 2. Preparation of polyindoles by EP.

3.2.2. D-A Polymers Synthesized by EP

Recently, D-A polymers have been used in SC devices to serve as both positive and negative charge storage materials. The D-A design has been widely used for developing low and high-bandgap conjugated polymers because the solubility, optical, HOMO/LUMO levels, and redox properties of the polymers can be optimized by tuning the donor and acceptor moieties and the side chains.[31,91–93] Their capacity to grasp both positive and negative charge (ambipolar doping properties) makes them suitable for energy storage devices.

The EP method has also been used to prepare D-A ambipolar conjugated polymers (Figure 6). Reynolds et al.[46] developed a D-A conjugated polymer, **P18**, using EDOT as a donor and isoindigo (iI) as an acceptor via EP where EDOT represents a p-dopable site and iI represents an n-dopable site. When **P18** was used as a p-dopable material for type I SC, a specific energy of 0.5 Wh kg^{-1} with retention of ≈80% of the electroactivity over 10000 cycles was achieved. On the other hand, in the type III device, where the polymer was used as both p- and n-dopable material, the polymer was operated in a high potential window of 2.5 V, and a higher specific energy of 15 Wh kg^{-1} was achieved although the device was less stable with ≈100% capacitance lost after 200 cycles owing to the instability of **P18** under negative bias.

Seferos et al.[94] also synthesized D-A polymers with one (**P19**) and two (**P20**) acceptor units and studied their performances. The two acceptor units enhanced negative charging stability and the ambipolar properties of **P20** while in **P19**, the negative charges were poorly delocalized. The type III SC device made from **P19** achieved a peak capacitance of 201 F g^{-1} with specific energy and specific power of 11 Wh kg^{-1} (at 0.5 A g^{-1}) and 20 kW kg^{-1} (at 50 A g^{-1}), respectively, while the device derived from **P20** attained a peak capacitance of 91 F g^{-1} with a specific energy of 4.8 Wh kg^{-1} (at 0.5 A g^{-1}) and high specific power of 55 kW kg^{-1} (at 50 A g^{-1}).

Polymer electrode materials with a porous network structure can afford appropriate channels for electrolyte counterions during doping/dedoping process and enhance the cycling stability of the material. In this regard, EP is a promising method to fabricate polymer electrode materials with porous 3D networks. As a representative example, Meng et al.[95] developed

a "chain–lock" design strategy to prepare a porous conjugated polymer **P22** from 4,7-bis(2,3-dihydrothieno[3,4-*b*][1,4]dioxin-5-yl)benzo[*c*][1,2,5]thiadiazole (DEBT) as the "chain" and tris(4-(2,3-dihydrothieno[3,4-*b*][1,4]dioxin-5-yl)phenyl)amine (TETPA) as the "lock" by electrochemical copolymerization. The lone pair of electrons in the N (sp^3) of TETPA that occupy the tetrahedral position creates a nonplanar structure and leads to the porous structure of the **P22** polymer electrode. **P22** exhibited pseudocapacitive properties and ambipolar doping ability with good performance in the p-doped state and attained an areal capacitance of 151.2 mF cm^{-2}, which is much higher than that of **P21** (65 mF cm^{-2}). Due to its porous network structure, **P22** delivered a high C_s of 149 F g^{-1} and cycling stability with 100% retention of the capacitance after 2000 cycles in the p-doped state.

Xu et al.[96] incorporated 3,4-dihexyloxythiophene as a π-spacer into a D–A–D molecular skeletons and synthesized the D–π–A–π–D-type polymer **P23**. The π-spacer created a porous morphology and facilitated ion diffusion, resulting in higher capacitance and electrochromic properties as compared to the polymer without the π-spacer. The CV of **P23** showed non-diffusion-controlled (pseudocapacitive) behavior. The polymer delivered a capacitance of 92 F g^{-1} at 1 A g^{-1} maintaining 90% of the original capacitance after 1000 cycles. In addition, when charged from −0.2 to 1 V, the polymer film changed from light blue to deep green with 46% optical contrast in the visible region and 271 cm^2 C^{-1} of coloration efficiency.

Ma et al.[97] employed the EP technique to prepare a linear polymer **P24** with a D-A–D structure and a branched polymer **P25** with polycarbazole as the main chain and anthraquinone as the side chain. Symmetric (type I) SC devices based on **P24** and **P25** electrodes exhibited pseudocapacitive behaviors and reached maximum cell voltages of 2.4 and 2.0 V, respectively. The **P24**-based device attained a maximum E_D of 29.1 Wh kg^{-1} at the P_D of 1.3 kW kg^{-1} while the **P25** device provided a maximum E_D of 19.5 Wh kg^{-1} at the P_D of 1.2 kW kg^{-1}. The study found that the charge-trapping effect during the doping process is the main cause of performance degradation. As compared to **P24**, **P25** exhibited a lower charge-trapping effect during the n-doping process and better cycling stability (retained 83% of original capacitance after 2000 cycles), which is ascribed to its extended conjugated structure, sparse morphology, and high p- and n-doping levels.

Recently, D–node–A (D–n–A)-type polymers containing "node" structures between the D and A moieties received more attention for SCs application owing to their unique properties.[98] The "node" such as sp^3 carbon atom(s) isolates the energy level, i.e., the HOMO is entirely located on the D units while the LUMO level is entirely located on the A units, as compared to D-A-type polymers. This allows for a change in the oxidation and reduction properties of the polymers by attaching substituents on the D and A units independently. Xie et al.[99] developed D–n–A-type cross-linked polymers **P26-P28** consisting of oligo-thiophene connected with tetrachlorinated perylene diimide (PDI) units via the "N node" by EP (Figure 6). All polymers presented two reversible redox behaviors corresponding to the redox couples of PDI/PDI^- and PDI^-/PDI^{2-} while the redox signal of the oligo-thiophene depends on the number and connection mode of the thiophenes. Furthermore, the polymers displayed non-diffusion-controlled redox reactions for both n-doping and p-doping processes. Among the polymers, **P27** showed balanced ambipolar features and a C_s of 299 F g^{-1} (271 F cm^{-3}) for the n-doping process and 264 F g^{-1} (258 F cm^{-3}) for the p-doping process due to easy ion diffusion and fast electron transfer as compared to the other polymers. Seferos et al.[100] also reported the D–n–A-type ambipolar polymer **P29** containing asymmetric tetrachlorinated PDI attached with a branched alkyl chain and EDOT monomer. **P29** exhibited balanced charge storage and good stability in both positive and negative regions and maintained more than 80% of its capacitance over 1000 cycles. The polymer films delivered moderate C_s of 78.6 F g^{-1} in the positive region and 73.1 F g^{-1} in the negative region at 0.5 A g^{-1} with rate capabilities of 87% and 56% in the positive and negative charge storage regions, respectively, at 20 A g^{-1}. Asymmetric (type III) SC device based on the ambipolar polymer **P29** with a gel polymer electrolyte achieved a wide cell voltage of 2.2 V, a maximum E_D of 8.95 Wh kg^{-1} at 1 A g^{-1} and a P_D of 76.8 kW kg^{-1} at 100 A g^{-1}.

Overall, the EP method has been utilized to prepare homopolymer- and D-A polymer (p-type and ambipolar)-based electrodes that showed C_s up to 990 F g^{-1} in half cells and 640 F g^{-1} in symmetric SCs.[74,76] The electrodes made by EP can be directly used for SCs unlike those prepared by chemical polymerization, which requires additional steps to fabricate an electrode by using non-conductive binders that usually decrease the performance and increase the overall cost of the devices. Although EP is a one-step and simple method, it is very monomer-selective. Especially monomers with too high oxidation potential cannot be electropolymerized and controlling and determining the molecular weights of the polymers is difficult.[94] The reproducible formation of polymers with identical redox and structural properties using EP is also challenging; even slight variations in temperature, applied potential, or monomer concentration can have a significant impact.[62] It is also a self-limiting process, where continuous polymerization would be suppressed if poorly conductive monomers are deposited on the current collectors.[101] Moreover, the electrical conductivities of polymers prepared by EP are relatively low compared to those prepared by other methods since highly conductive substrates like metals, carbons, and metal oxides are required as electrodes for the polymerization. Using the EP method to prepare nanostructured composite electrode materials also presents difficulties, since achieving controlled electrochemical deposition of different materials could be challenging.

3.3. Chemical Polymerization

As an alternative to EP, chemical polymerization has been widely employed to make polymers and their composites for capacitor applications. Chemical polymerization is a polymerization technique that occurs by oxidation of the monomers or transition metal-catalyzed cross-coupling reactions. In chemical oxidation polymerization, the monomers are oxidized using an oxidizing agent like ammonium persulfate and ferric chloride which have been employed to synthesize some homopolymers like polyaniline and polypyrrole. For example, Wu et al.[102] developed a nanostructured PANI/reduced graphene oxide (rGO) composite gel by a solution-assisted two-step self-assembly method

from graphene oxide (GO) and chemically polymerized PANI. The PANI/rGO composite electrode exhibited a high C_s of 824 F g^{-1} (5830 mF cm^{-2}) at a current density of 2.22 A g^{-1} (15.72 mA cm^{-2}) and an outstanding rate performance due to the good morphology that facilitated the diffusion of the electrolytes and transport of the electrons in the composites. Chemical polymerization by transition metal-catalyzed cross-coupling reactions involves the coupling of the monomers in the presence of a metal catalyst. Typical examples include Suzuki polymerization, Stille polymerization, and direct (hetero)arylation polymerization (DHAP). This method allows for the synthesis of solution-processable p-type and n-type polymers, which can be easily spray-coated and spin-coated on a flexible and transparent conducting substrate such as ITO-coated polyethylene terephthalate (PET) and processed by roll-to-roll printing.

3.3.1. p-Type Polymers Synthesized by Chemical Polymerization

In this section, p-type polymers, mainly those synthesized by transition metal-catalyzed cross-coupling reactions, will be discussed. The structures of some p-type polymers synthesized by chemical polymerization are shown in **Figure 7**.

Chemical polymerization techniques, particularly the Stille polycondensation, and direct (hetero)arylation polymerization, have been utilized for the synthesis of p-type polymers (Figure 7). Unalan et al.[103] employed the Stille polymerization to synthesize poly(4-(dithieno[3,2-*b*:2′,3′-*d*]thiophen-2-yl)-2-(2-octyldodecyl)-2*H*-benzo[*d*][1,2,3]triazole) (**P30**) for electrochromic SC electrodes. The electrodes made from the composite of this polymer and single-walled carbon nanotube (SWNT) by physical blending showed pseudocapacitive characteristics, multiple color changes, and a C_s of 112.4 F g^{-1} at 1 A g^{-1} with 82% capacity retention after 12500 cycles.

Meng and coworkers[70] synthesized the solution-processable polymer **P31** using direct DHAP. **P31** showed a color change from green to blue during charging/discharging, which makes it useful for hybrid applications. The **P31**/ITO/PET electrode showed an areal capacitance of 2.5 mF cm^{-2} and a C_s of 31 F g^{-1} at a current density of 0.1 mA cm^{-2}. The type IV device fabricated using **P31** as a positive electrode and PEDOT as a negative electrode gave a wide potential window of 1.4 V with a near-ideal rectangular-shaped CV curve (pseudocapacitive property) and a high E_D of 6.3 Wh kg^{-1} at 0.8 A g^{-1} as compared with the type I devices.

Although PEDOT is extensively used as positive and negative electrodes in SCs, its application for large-area commercial SCs is limited because it is insoluble in the absence of surfactants and dispersants and hence is usually prepared by electropolymerization. Reynolds et al.[104] reported the soluble dioxythiophene polymers **P32** and **P33** which are electrochemically equivalent to PEDOT. The polymers were synthesized by the DHAP of alkoxy-functionalized 3,4-propylenedioxythiophene (ProDOT) with EDOT. **P32** and **P33** were incorporated in SCs and presented similar pseudocapacitive features, capacitance, voltage, and stability to that of electrodeposited PEDOT. The type I SCs constructed from these polymers achieved cell voltage up to 1.6 V, E_D up to 18 Wh kg^{-1}, and P_D up to 3.3 kW kg^{-1} along with less than 20% loss of capacitance after 50000 cycles.

The type, size, and polarity of the side chain affect the redox properties and hence conductance and capacitance of a conjugated polymer. Reynolds and co-workers[105] investigated the effect of side chains on the capacitance and redox properties of conjugated polymers with various side chains (Figure 7). The polymers were synthesized by the co-polymerization of ProDOT functionalized with various side chains at the 2-position of the propylene bridge with 3,3-dimethyl-3,4-dihydro-2*H*-thieno[3,4-*b*][1,4]dioxepine (DMP) using the DHAP technique. They found that the bulky side chains in **P38** resulted in poor electrochemical accessibility, low conductance, increased charge transfer resistance at high doping levels, and low specific mass capacitance (52 F g^{-1}). On the other hand, **P34**, containing linear (n-octyl) side chains, showed better electrochemical accessibility initially but oxidation of the polymer occurred more slowly leading to lower specific mass capacitance (82 F g^{-1}) than that of its branched-chain counterpart **P35** (R = 2-ethylhexyl, 113 F g^{-1}). **P35** with shorter branched alkyl chains gave the highest charge capacity and specific capacitance per mole repeat unit which are higher than for **P34**, **P36**, and **P37**. Furthermore, **P39**, functionalized with a polar oligoether side chain, afforded a C_s of 82 F g^{-1} in an aqueous electrolyte and 84 F g^{-1} in an organic electrolyte and showed full colored-to-colorless optical transitions with electrochromic contrast (Δ%T > 70%).[106] These studies indicate that the type and length of the side chain on the polymers can clearly influence potential window, doping level, electrochemical accessibility of the redox sites, pseudocapacitance, and charge transfer resistance.

Electrochemically stable, and processable PANI-derivatives **P40** and **P41**, synthesized by Buchwald/Hartwig coupling reaction from carbazole and 1,4-aryldiamines, were reported by Scott et al.[107] **P40** showed high conductivity (2.8 S cm^{-1}) due to its larger molecular weight compared to **P41** (0.70 S cm^{-1}). The spray-coated **P40** showed reversible color change during electrochemical cycling and a maximum areal capacitance of 64.8 mF cm^{-2} and a C_s of 319 F g^{-1} at a current density of 0.2 mA cm^{-2} (half-cell) with 83% capacitance retention after 1000 cycles. The all-polymer symmetric (type I) SC based on **P40** revealed CV curves with a combination of both pseudocapacitive and EDLC properties and gave an E_D of 2.45 Wh kg^{-1} at a P_D of 2.71 kW kg^{-1} with over 91% capacitance retention after 1000 cycles, which is comparable with similar type I PANI devices.

Electrochromic SCs based on D-A polymers have been explored since the charge storage capacity and electrochromic properties can be adjusted by tuning the donor and acceptor units and the side chains on the polymers. Unlike the EP method, chemical polymerization permits the synthesis of D-A polymers by combining various donor and acceptor units. Recently, three twisted ladder-like polymers **P42**, **P43**, and **P44** were synthesized from twisted spirobifluorene and linker units including indacenodithiophene (IDT), benzothiadiazole (BT) and diketopyrrolopyrrole (DPP), respectively (Figure 7).[108] As a result of separated HOMO/ LUMO wave functions, i.e., separated p-doped and n-doped sites, **P42** showed a higher areal C_s of 6.2 mF cm^{-2} during the p-doping process, and 2.4 mF cm^{-2} during the n-doping process, color changes and better stability than **P43** and **P44**. The asymmetric SC with **P42** as the anode material and $W_{0.71}Mo_{0.21}O_{3-x}$ as the cathode material gave an areal C_s of 1.38 mF cm^{-2} and an E_D of 3.89 Wh kg^{-1}.

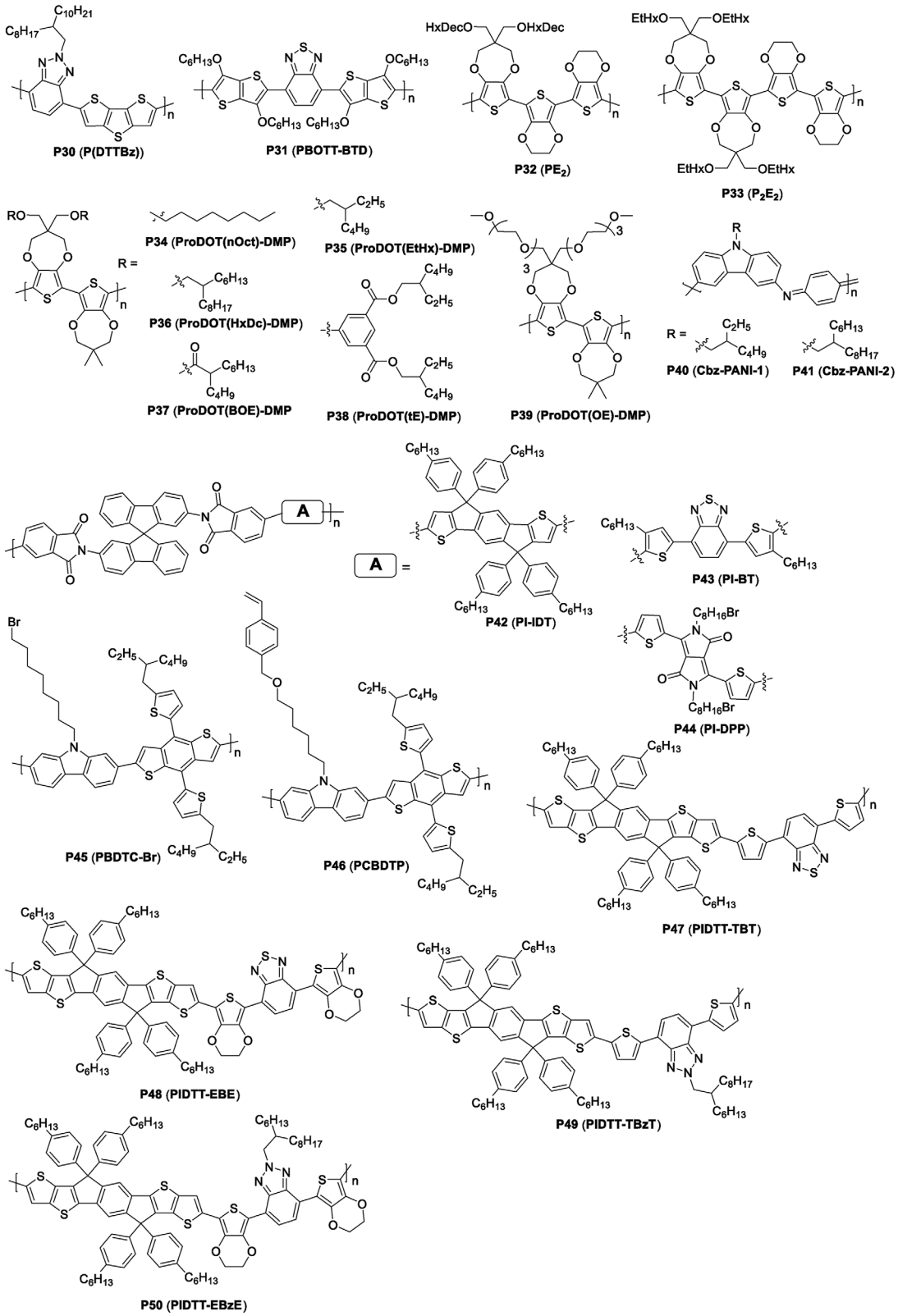

Figure 7. Chemical structures of p-type polymers synthesized by chemical polymerization.

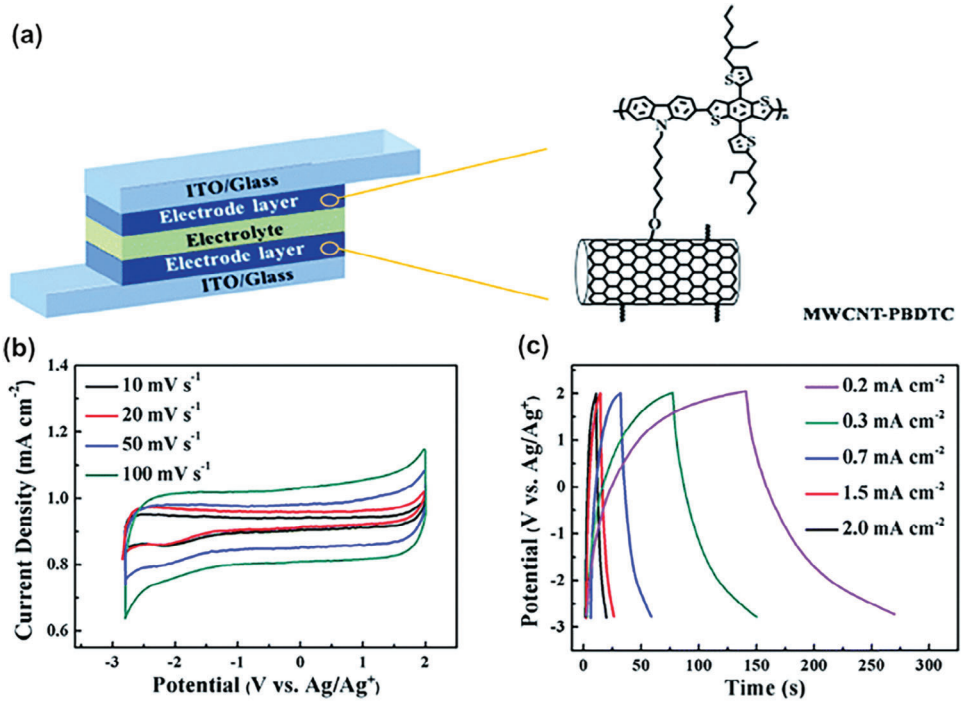

Figure 8. Schematic of electrochromic SC device and the structure of MWCNT–**P45** a), CV b), and GCD c) curves of the symmetric SC. Reproduced with permission.[109] Copyright 2018, The Royal Society of Chemistry.

Conjugated polymers show promising electrochromic properties; however, their low energy density and poor electrochemical stability limit their application in bifunctional electrochromic SCs. In recent years, many endeavors have been devoted to improving these properties. One of the strategies that have been used to improve these properties was developing p/n-dopable composite electrode materials. Guo et al.[109] developed solution-processable p/n-dopable composite electrodes from hydroxylated multi-walled carbon nanotubes (MWCNT-OH) and **P45** using Williamson ether reaction. **P45** was synthesized from carbazole and benzodithiophene by the Stille polymerization reaction. The composite electrode showed reversible redox features over a wide potential window and a capacitance of 175 F g^{-1} in a half cell (**Figure** 8a). The shapes of the CV curves of MWCNT–**P45** indicate the contribution of both the electric double layer of the MWCNT and the pseudocapacitive (Faradaic) character of the polymer redox reaction. The MWCNT–**P45** film-based solid-state electrochromic symmetric SC exhibited a high E_D of 174.7 Wh kg^{-1} with a very wide potential window of 4.8 V using 0.5 M $LiClO_4$/PC as electrolyte (Figure 8b). This high E_D was ascribed to efficient electron transport between the highly conductive MWCNT and **P45**, which enhanced charge storage and promoted electron and ion transport during the charge/discharge cycle. The device showed high stability with 4% capacitance loss after 5000 cycles and reversible color change from brown (discharged state) to gray (charged state) with high optical contrast.

It has been found that cross-linked polymers enhance the mechanical and morphological stability of the polymer electrodes by decreasing the swelling and shrinkage of the polymer that arises during the charging/discharging process.[110,111] Very recently, Lin et al.[112] synthesized **P46**, which contains carbazole and benzodithiophene in the main chain and pendant styryl group on the side chain, to improve the stability and processability of the polymer. This polymer was crosslinked thermally to give the hyper crosslinked polymer **PCBDTP-X** and used as a positive electrode, with PEDOT as a negative electrode, to fabricate all-polymer electrochromic type IV SCs (**Figure** 9a). The use of a polymer-based solid electrolyte realized an E_D of 18.4 Wh Kg^{-1} with an operating potential of 2.4 V. More importantly, **PCBDTP-X** achieved good cycling stability with retention of 99.1% of the original capacitance after 5000 cycles as compared to the non-crosslinked **P46**. Furthermore, the color of the asymmetric device changed reversibly from yellow-brown to gray-blue (Figure 9b).

Wang et al.[113] prepared the electrochemically stable polymers **P47-P50** by copolymerizing indacenodithieno[3,2-*b*]thiophene (IDTT) with four different D-A-D units which have more polar EDOT or less polar thiophene as donors and benzo[*c*][1,2,5]thiadiazole or benzo[*d*][1,2,3]triazole as acceptors. The polymers presented strong optical absorption while characteristically different colors due to differences in D-A-D units and changes in the intramolecular charge transfer in the polymer backbone. At a higher scan rate (100 mV s^{-1}), **P47**, **P48**, **P49**, and **P50** delivered C_s of 150, 110, 160, and 190 F g^{-1} (half-cell), respectively. Among the polymers, **P50** exhibited the highest C_s of 260 F g^{-1} at 5 mV s^{-1}, which is attributed to the strong polymer-electrolyte interaction and efficient electrochemical doping of the polar backbone (>100%).

The polarity of a polymer film needs to be optimized to minimize the hydrophobic properties that arise from alkyl side chains to ensure compatibility with aqueous-based electrolytes. In this regard, Reynolds et al.[114] used DHAP to prepare a polymer containing EDOT and a ProDOT derivative with ester-functionalized

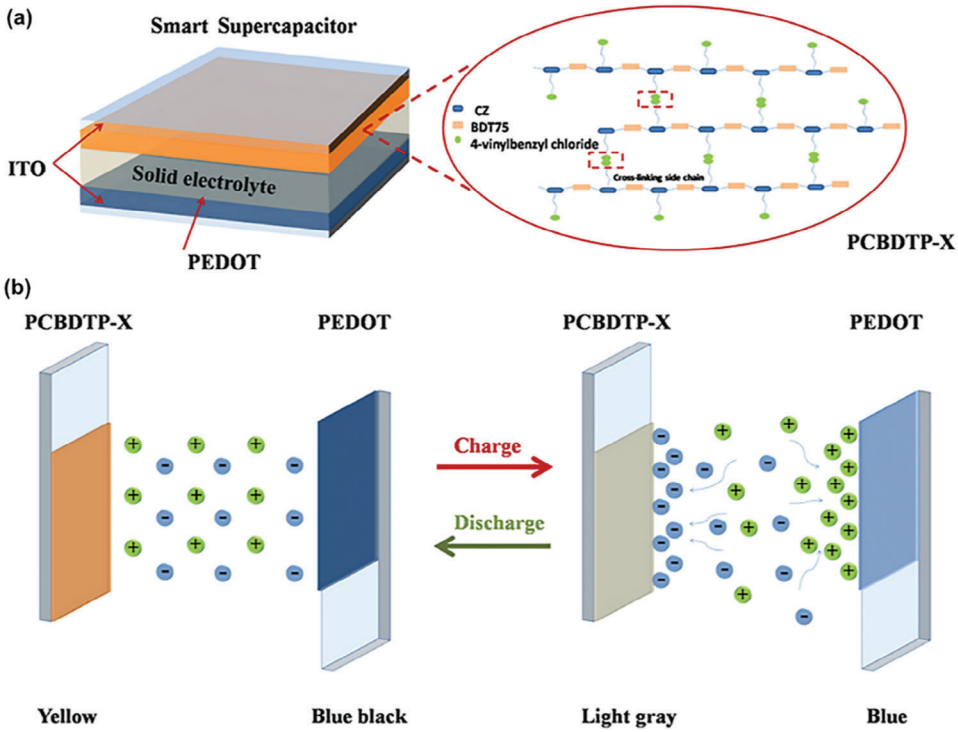

Figure 9. The structure of the PCBDTP-X-based asymmetric SC device a), and the color change during the charge/discharge process b). Reproduced with permission.[112] Copyright 2020, Elsevier.

side chains (**Scheme 3**). This organic-soluble polymer was transformed into a water-soluble conjugated polyelectrolyte (PE) containing carboxylate groups by base-catalyzed hydrolysis of the ester functional groups. Further washing of the polymer film with a mild acid gave solvent-resistant polymer films that were compatible with both organic and aqueous device electrolytes. The solvent-resistant polymer film exhibited pseudocapacitive properties and comparable C_s in both LiBTI/H_2O (42 F g^{-1}) and NaCl/H_2O (33 F g^{-1}) at 50 mV s^{-1} in a half cell while the type I SC delivered a C_s ≈18 F g^{-1} with retention of 75.3% of the C_s after 1 75000 cycles using 0.5 M NaCl/water as the device electrolyte.

3.3.2. n-Type Polymers Synthesized by Chemical Polymerization

While several high-performance p-type polymers were designed and synthesized for energy storage applications, there are only a limited number of prominent n-type polymers. One of the reasons is that polymer electrodes are less stable in their n-doped state in the presence of oxygen and water, which further restricts their application in aqueous electrolytes.[97] In addition, developing stable n-type polymers with high mobility for high-performance SCs is challenging because electron-deficient monomers with suitable high electron affinity and high ionization energies are scarce. However, n-type polymers are crucial for enhancing the potential window and energy density of SCs by combining them with p-type polymers and fabricating asymmetric SCs. n-Type polymers synthesized by chemical polymerization are shown in **Figure 10**.

1,4,5,8-Naphthalenediimide (NDI)-based conjugated redox polymers have been explored as n-type polymers for energy storage applications.[115] Recently, Liang et al.[116] used NDI-based acceptor polymers **P51** and **P52**, which have been widely used in all-polymer solar cells,[117] for energy storage applications. The **P51** electrode showed relatively stable and reversible n-dopability at a high doping level in organic electrolyte with a specific capacity of 54.2 mAh g^{-1} and a 96% capacity retention after 3000 cycles as compared to **P52** (specific capacity 47.4 mAh g^{-1}) with π-insulating ethanyl group.

Asha and coworkers[118] synthesized n-type D-A polymers containing NDI as the acceptor and thiophene-terminated phenylenevinylene as the donor by DHAP. The type III SC fabricated using a composite of carbon nanotubes and the polymer as an electrode and H_2SO_4 as the aqueous electrolyte showed a rectangular CV curve and a slightly distorted GCD curve which are characteristic behaviors of pseudocapacitive materials. The device with **P53**, the polymer with cyano groups at the vinylene linkage, presented a C_s of 124 F g^{-1} with good stability and almost 100% retention of the initial capacitance after 5000 cycles. However, the polymer without the cyano groups (**P54**), and the reference polymer (**P51**) attained low C_s of 84 and 61 F g^{-1}, respectively. The same group[119] also investigated the charge storage capacity of D-A alternating (**P55**, **P56**) and random (**P57**, **P58**) polymers which were synthesized by the Stille polymerization from NDI or PDI as the acceptor unit and benzodithiophene (BDT) as the donor unit. The irregular arrangement of the donor and acceptor units in the random polymers resulted in reduced homogeneity in the polymer chains and thereby attained lower charge storage capacity than the alternating polymers. **P56** possessed a

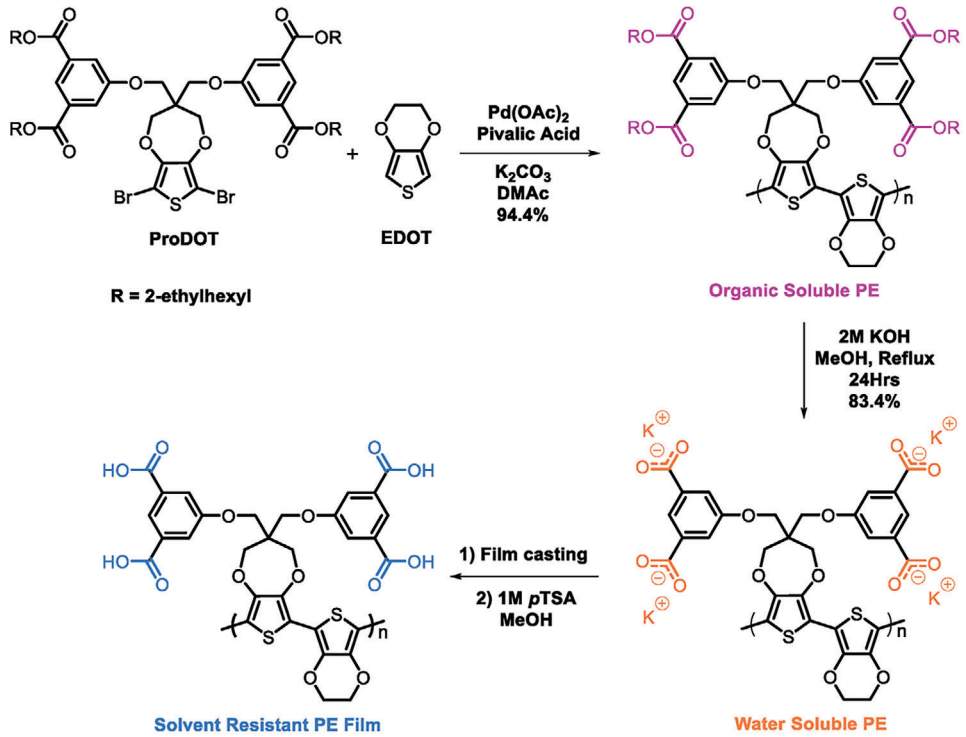

Scheme 3. Synthetic routes of a solvent resistant polymer film. (adapted from Ref. [114])

high C_s of 113 F g^{-1} with almost 100% retention of the original capacitance after 4000 cycles.

The performance of n-type polymers is adversely affected by high charge transfer resistance. In addition, their decay is rapid due to the instability associated with strong charge localization.[97,120] To address this issue, Azoulay et al.[121] developed the low bandgap open-shell D-A conjugated polymer **P59** from cyclopentadithiophene donor and thiophene-substituted thiadiazoloquinoxaline acceptor. It displayed strong internal charge transfer between the donor and acceptor units, high charge delocalization in the reduced state, and pseudocapacitive property. The symmetric (type I) SC fabricated with **P59** demonstrated good reversibility and cycling stability, retaining 90% capacitance after 2000 cycles. In the case of asymmetric (type IV) SC, with **P59** as the anode and PEDOT:PSS as the cathode electrode, operated at a wide voltage window of 3 V, gave a maximum E_D of 30.4 Wh kg^{-1} at 1 A g^{-1} discharge rate and a P_D of 14.4 kW kg^{-1} at 10 A g^{-1} discharge rate. Furthermore, the asymmetric SC presented 85% capacitance retention, whereas the symmetric one showed 79% retention after 5000 cycles.

Polybenzimidazobenzophenanthroline (**P60**) is another n-type polymer that received attention for SC application. One of the interesting features of this ladder-type polymer is its high electrical conductivity of 2.4 S cm^{-1} upon n-doping, which is three orders of magnitude higher than **P51** (5×10^{-3} S cm^{-1}).[122] The high conductivity is due to the high rigidity and planarity of the polymer backbone, which facilitates the delocalization of the charge carriers and makes intramolecular charge transfer easier. Thus, **P60** has been used as n-type material for solar cells, field-effect transistors, and energy storage devices.[123,124] Recently, Crispin et al.[125] used **P60** as the anode and **P62**, with a polar side chain (**Figure 11**), as the cathode to fabricate all-polymer asymmetric (type IV) SCs that operate in a potential window up to 1 V in aqueous electrolytes. Both polymers showed pseudocapacitive behaviors in half cells and **P60** attained a C_s of 226 F g^{-1} while the C_s for **P62** was 113 F g^{-1}. The **P60**/**P62** SCs achieved areal capacitances of 90 mF cm^{-2} and C_s of 33 F g^{-1} with excellent stability and almost 100% capacitance retention after 10000 cycles.

Yang et al.[126] reported **P61** derived from perylene-3,4,9,10-tetracarboxylic dianhydride as a monomer and 2,6-diaminoanthraquinone as a linker by condensation reaction. The polymer achieved a C_s of 245 F g^{-1} at 5 mV s^{-1} in a negative potential range in 1 M H_2SO_4 electrolyte and a capacitance retention of 36.7% after 5000 cycles. The C_s further improved to 604 F g^{-1} at 5 mV s^{-1} (659 F g^{-1} at 1 A g^{-1} from GCD) when **P61** was modified on rGO (**P61/rGO**). The charge storage for both **P61** and **P61/rGO** is mainly a capacitive-controlled reaction (pseudocapacitive property). When **P61/rGO** was integrated into an asymmetric SC as a negative electrode, it gave a C_s of 125 F g^{-1} at 1 A g^{-1} with energy storage of 19.8 Wh kg^{-1} at 570 W kg^{-1} and maintained 71.8% of the capacitance over 1 0000 cycles.

It was found that attaching hydrophilic polar side chains such as oligo(ethylene glycol) (OEG) moieties on the polymer backbone provides an advantage over hydrophobic alkyl side chains to fabricate aqueous-based organic electronic devices such as solar cells and energy storage devices.[127,128] Recently, Nelson et al.[129] synthesized a p-type homopolymer **P63** from 3,3′-OEG-substituted bithiophene and n-type D-A polymers **P64** and **P65** from 3,3′-OEG-substituted bithiophene and NDI with zwitterionic and OEG side chains, respectively (Figure 11). **P63** showed

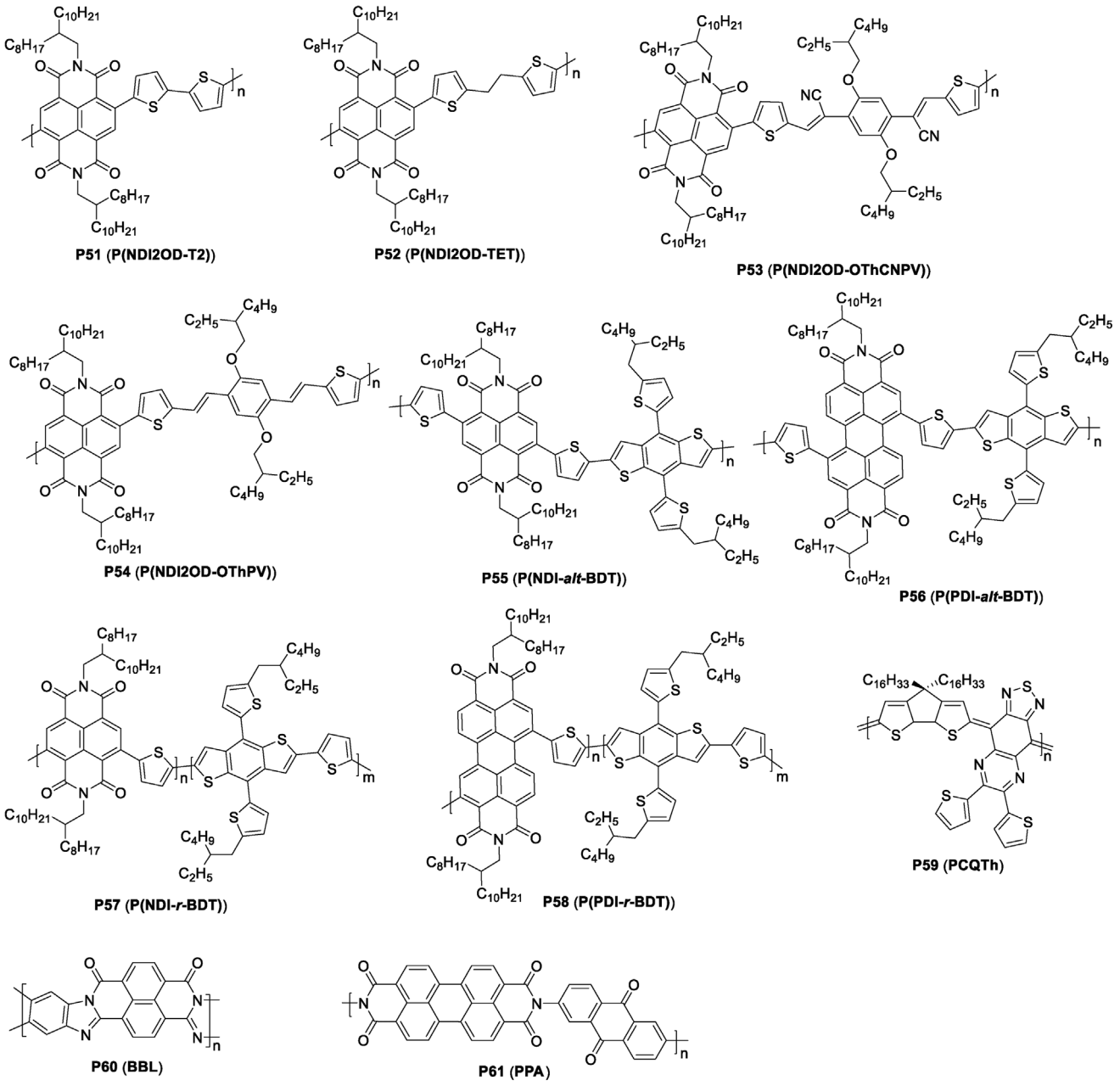

Figure 10. Chemical structures of n-type and n/p-type polymers synthesized by chemical polymerization.

fast charging due to the efficient hole (hole mobility up to 0.95 cm^2 Vs^{-1}) and ionic transport properties in the film. Both **P63** and **P64** revealed fast and reversible charging and achieved gravimetric capacities of 21.3 and 25.9 mAh g^{-1}, respectively. **P64**, the n-type polymer with zwitterionic side chains, possessed a higher specific capacity (more than three times) than **P65** with OEG side chains. When **P63** and **P64** were assembled in a two-electrode cell, output voltages of up to 1.4 V (in NaCl aqueous electrolyte) with high redox stability were obtained. This study revealed that the polymer backbone controls the stability, redox potential, and electronic transport, while the polar side chain influences the ionic mobility, charging rate capability, and capacity.

Very recently, Peurifoy et al.[42] developed an n-type polymer **P66** (perylene diimide–hexaazatrinaphthylene) based on two design rules for high energy storage, rate capability, and long-term stability, which are, i) the combination of complementary electroactive units, and ii) molecular contortion to allow both facile diffusion and long-range charge delocalization (**Figure 12**). **P66** was synthesized from PDI and hexaazatrinaphthylene (HATN) via Suzuki cross-coupling followed by photocyclization. The CV of **P66** showed broad and reversible reduction peaks which revealed pseudocapacitive and battery-like behaviour. As depicted in Figure 12, the charge-storage mechanism of **P66** involved accepting two electrons first by the PDI unit, and then two more

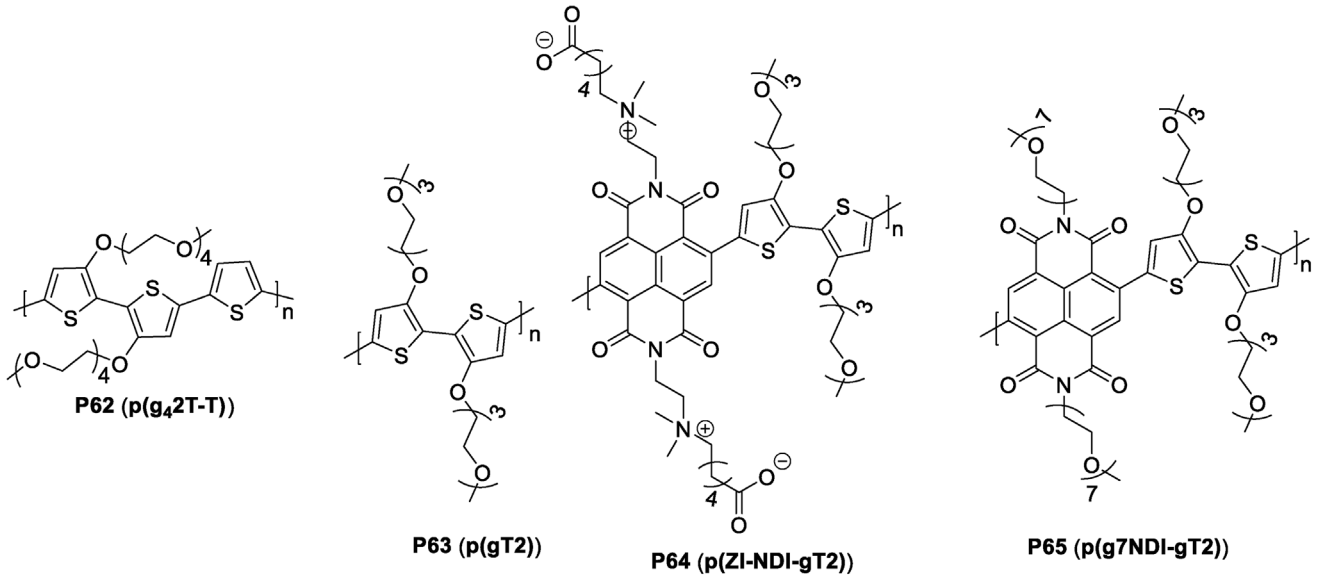

Figure 11. Chemical structures of p-type and n-type polymers with polar side chains.

electrons by the HATN moiety. **P66** attained a high C_s of 689 F g^{-1} at a current density of 0.5 A g^{-1} in a half cell and performed well even at very high current densities (75 A g^{-1}), yielding a C_s of over 430 F g^{-1}. These values are the highest among those reported for n-type polymer pseudocapacitor materials. Interestingly, the polymer retained 92% of the initial capacitance after 5 0000 cycles in a half cell.

In general, chemical polymerization methods, particularly Stille and DHAP, are promising to develop p-type and n-type polymers with different backbone structures and properties. Moreover, the methods allow the preparation of D-A polymers by combining various donor and acceptor units and engineering the side chains to improve the potential window, energy density, electrochromic properties, stability, and processibility for large-scale production. With n-type polymers made by chemical polymerization, C_s up to 689 F g^{-1} with high cycling stability up to 50000 cycles in half cells and C_s up to 125 F g^{-1} for asymmetric devices were achieved. However, most of these polymer-based SCs still delivered low C_s and energy density as compared to the state-of-the-art nanostructured composite electrode materials, which need further development of new design rules. Furthermore, the chemical polymerization method has disadvantages including not being atom-economic and eco-friendly with the use of toxic transmetallating reagents like alkylstannanes used for Stille polymerizations.[130] Increased synthetic steps and cost are other limitations of this method. To make this polymerization method more eco-friendly, emerging chemical polymerization methods, especially direct arylation polycondensation, and aldol condensation polymerization, can be utilized to develop electrode materials for SCs.

3.4. In Situ Polymerization

The performance and stability of conjugated polymer-based electrodes in energy storage can be further improved by forming nanostructured composite materials through modification of the polymer structure and incorporation of other functional moieties.[131] The nanostructured conjugated polymers have large surface area, short charge transport paths, and better electrical, electrochemical, and mechanical properties than the pure

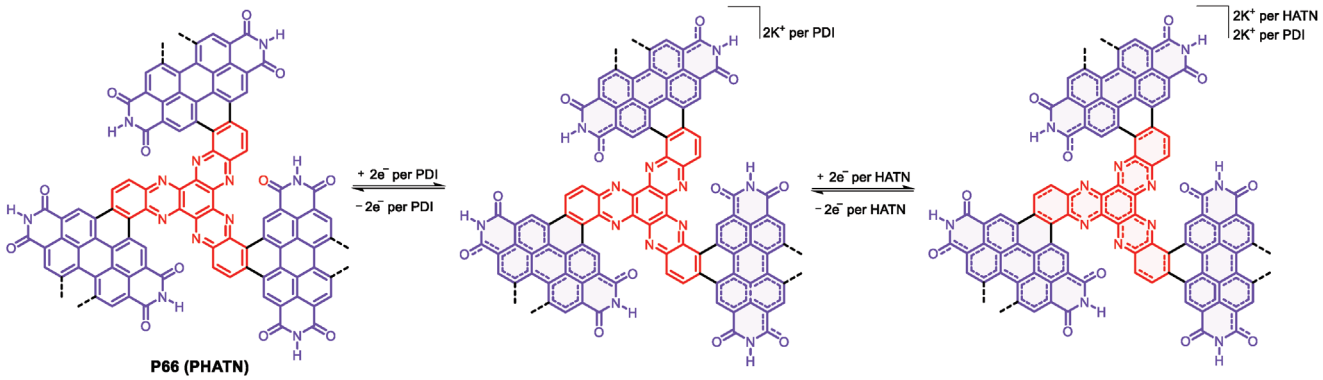

Figure 12. Structures and charge storage mechanism of **P66** (PHATN). (adapted from ref. [42])

(bulk) conjugated polymers.[132] The conjugated polymers can be combined with carbon materials such as graphene, carbon nanotubes, activated carbons, cellulose and its derivatives, and metal oxides to get the nanostructured polymers. In situ polymerization has been used to prepare nanostructured polymer-based composite electrodes for SCs.[133,134] This technique involves mixing a neat solution of the monomer(s), followed by polymerization in the presence of either dispersed carbon materials/metal oxides or a current collector coated with carbon materials or metal oxides. It has advantages such as low cost, short reaction time, simplicity, and appropriateness for large-scale production of electrode materials for energy storage devices.[135,136] For example, in situ polymerization has been utilized to fabricate polymer electrodes on carbon paper current collectors, thereby enhancing the surface area, conductivity and ultimately improving the performance of the polymer electrodes. A superhydrophilic thin layer of PANI (PANI–Toray paper) was developed by in situ electropolymerization of PANI on electrochemically-modified Toray carbon paper.[41] The electrode material attained a high capacitance of 1700 F g^{-1} in a half cell and a C_s of 1335 F g^{-1} (areal capacitance of 1.3 F cm^{-2}) at 10 A g^{-1} in the solid-state symmetric SC. The device also delivered a high rate capability (1217 F g^{-1} at 50 A g^{-1}) and a high E_D of 30 Wh kg^{-1} at a P_D of 2 kW kg^{-1} with 85% retention of capacitance up to 10000 cycles. Hatton et al.[137] also improved the performance of PPy by developing nanostructured polymer hybrids, PVF/PPy, through simultaneous electropolymerization of pyrrole monomer and electroprecipitation of polyvinylferrocene (PVF) on carbon fiber paper. The PVF/PPy hybrid electrode attained a C_s of 514.1 F g^{-1}, which is significantly higher than those of PPy (27.3 F g^{-1}) and PVF (79.0 F g^{-1}) in a half cell because of the pseudocapacitance contribution from both PVF and PPy. The type I SC showed a C_s of 345.3 F g^{-1} and E_D of 25.4 Wh kg^{-1} at a P_D of 58.6 kW kg^{-1}, which is also higher than that of either PVF or PPy as a result of the facilitated ion diffusion in the hybrid (via the synergy of PPy and PVF). In general, in situ polymerization has been extensively utilized for fabricating binary and ternary composite electrodes incorporating polymers and other materials. The following sections describe high-performance polymer composites with 2D materials and biomolecules.

3.4.1. Polymer Composites with Metal Oxides, CNT, and Graphene

Binary and even ternary composite electrodes with high surface area and electrical conductivity have been fabricated by *in situ* polymerization, which achieved high capacitance in SC devices. The capacitance of PANI has been improved by forming a binary graphene/PANI nanorod composite by in situ electropolymerization of aniline monomer on graphene paper.[138] As a result of the synergetic effect of PANI and graphene, the free-standing and flexible composite showed a higher C_s of 763 F g^{-1} at a current density of 1 A g^{-1} and better cycling stability as compared to pristine PANI (520 F g^{-1}) and graphene paper (180 F g^{-1}). The performance of graphene/PANI was further increased by modifying the structure of the composite electrode (Pg^{-1}) to a phase-separated structure via electrochemical deposition of PANI onto graphene hydrogel monolith (GHG), as shown in **Figure 13**a.[139] The SEM image (Figure 13b-d) revealed that Pg^{-1} had a phase-separated structure where the GHG matrix (purple) was covered by a PANI layer (green). This phase-separated composite showed better diffusion of the electrolyte than the uniform composite, which resulted in a high C_s of 783 F g^{-1} at a larger current density of 27.3 A g^{-1} (high rate performance) and 791 A g^{-1} (8773 mF cm^{-2} mF cm^{-12}) at a lower current density of 1.14 A g^{-1}. The symmetric (type I) SC fabricated using the composite material also exhibited a high C_s of 712 F g^{-1} at 1.08 A g^{-1}.

The PANI nanoneedle arrays have also been coupled with MoS_2 thin nanosheets via in situ polymerization to get MoS_2@PANI architectures, which gave high surface area and electrical conductivity that facilitated fast transport/diffusion of charges.[140] The CV and GCD curves of MoS_2@PANI showed pseudocapacitive features. Interestingly, the symmetric SC derived from this material afforded a higher C_s of 853 F g^{-1} than pure PANI and MoS_2 at 1 A g^{-1} with a high E_D of 106 Wh kg^{-1} and P_D of 106 kW kg^{-1}.

Shirage et al.[141] developed nanocomposite Px-MWCNT/PANI through in situ polymerization of aniline in the presence of partially exfoliated MWCNT (Px-MWCNT) and compared its SC performance with Px-MWCNT and PANI using redox-active polymer gel as electrolyte and separator. Px-MWCNT/PANI exhibited a quasi-rectangular CV curve which is ascribed to the dominant pseudocapacitive and battery-type contribution of the redox-active hydroquinone in the electrolyte which adds extra Faradaic capacitance to the total capacitance. The symmetric SCs delivered high C_s of 186.1, 809.6, and 644.4 F g^{-1} at 25 mV s^{-1} for Px-MWCNT, Px-MWCNT/PANI and PANI, respectively, as compared with the device without redox-active hydroquinone as electrolyte. The high C_s of Px-MWCNT/PANI/-based device is attributed to the synergistic effect of Px-MWCNT and PANI, unique morphology, and highly redox-active hydroquinone in the gel electrolyte.

The performances of PANI and PPy have also been enhanced by forming a ternary nanocomposite MoS_2/PPy/PANI.[142] PPy was grown by in situ chemical oxidative polymerization of pyrrole monomer on the surface of MoS_2 and then aniline monomer was polymerized (in situ) on the surface of MoS_2/PPy that resulted in a "pizza-like" nanostructured ternary nanocomposite, which showed a higher performance than the pure and binary materials. As a result of the synergistic effect, MoS_2/PPy/PANI exhibited pseudocapacitive behavior and attained higher C_s of 1273 F g^{-1} (half-cell) at 0.5 A g^{-1} than those of MoS_2 (169 F g^{-1}), PPy (136 F g^{-1}), PANI (528 F g^{-1}), MoS_2/PPy (449.5 F g^{-1}), and PANI/PPy (784 F g^{-1}). Furthermore, MoS_2/PPy/PANI showed a high rate of performance (a C_s of 673 F g^{-1} at a high current density of 10 A g^{-1}) due to short ion diffusion paths and better electrical conductivity.

Ternary nanostructured PANI/Fe_2O_3-decorated graphene (PGF) composite hydrogel, made by in situ polymerization on the surface of Fe_2O_3-decorated graphene sheets was also reported by Ohlan et al.[40] The symmetric SC based on ternary PGF showed a high C_s of 1124 F g^{-1} at 0.25 A g^{-1} in 1 M H_2SO_4 and maintained its C_s of 923 F g^{-1} even at a higher current density of 7.5 A g^{-1}. The devices exhibited high cycling stability with a retention of 82% of the initial capacitance after 10000 cycles. The CV curve of the composite showed two pairs of broad redox peaks with a quasi-rectangular shape which indicates the pseudocapacitive behavior of the composites. The high performance and stability are mainly due to the coexistence of

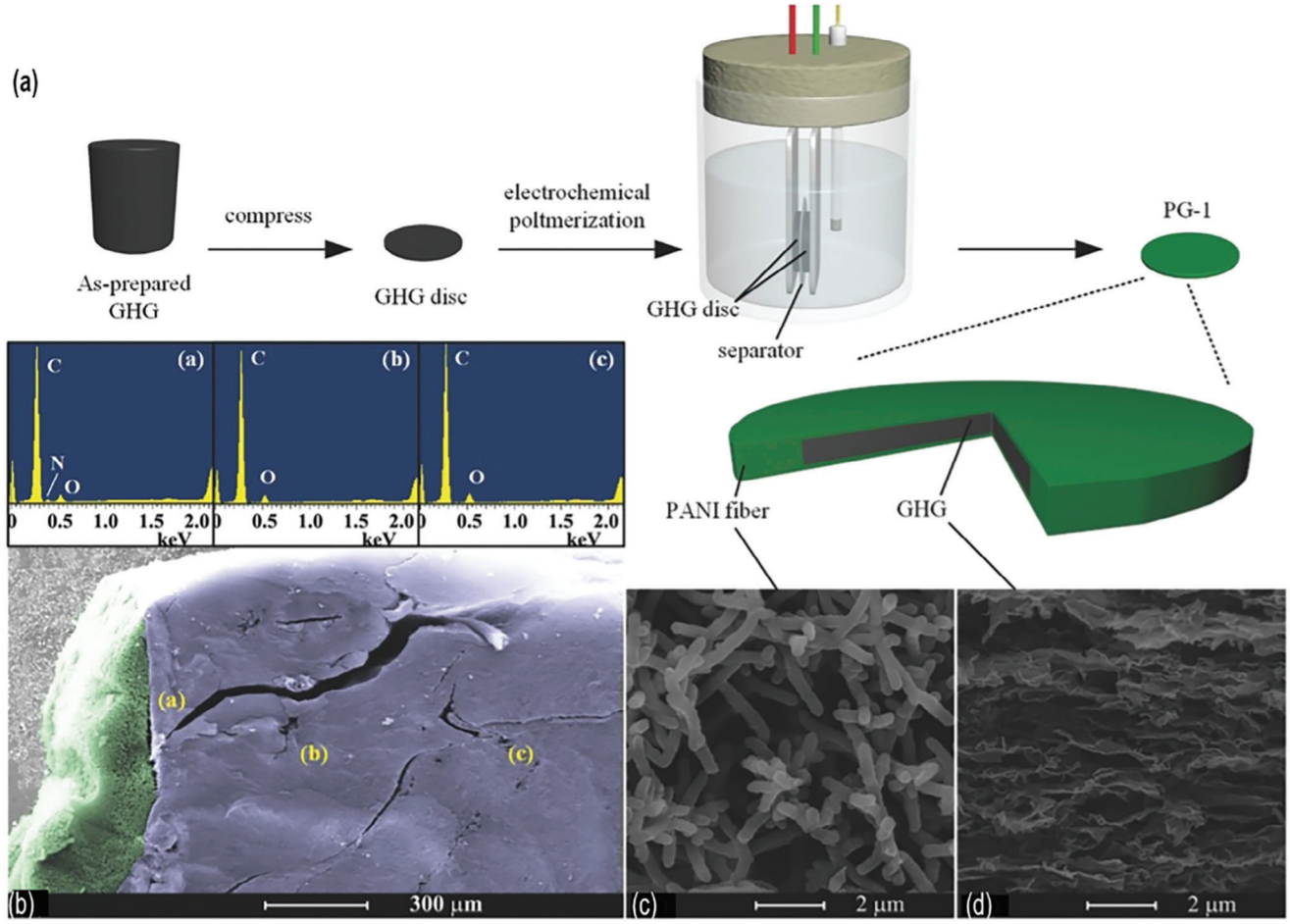

Figure 13. Schematic illustration for the preparation of Pg^{-1} a), cross-sectional SEM image of Pg^{-1} b), SEM image of the PANI cap layer in Pg^{-1} c) and SEM image of the GHG matrix in Pg^{-1} d). Reproduced with permission.[139] Copyright 2016, John Wiley & Sons.

PANI over the Fe_2O_3-decorated rGO, which increased the electrical conductivity, promoted the rapid penetration of electrolyte and ion permeation, and reduced the charge transfer distance. The above results indicate that the PANI-based composite electrodes prepared by in situ polymerization show much higher C_s than the pristine polymer, making the polymerization method effective for developing high-performance electrodes.

Sulaiman et al.[143] developed a free-standing bilayer composite film r-PGMGN (PPy/rGO/MWCNT/rGO/NCC) by layering MWCNT/rGO/nanocrystalline cellulose (NCC) composite on PPy/rGO composite layer prepared by in situ polymerization. The symmetric SC based on the free-standing film of r-PGMGN exhibited both pseudocapacitor and EDLC features. The device showed a high C_s of 882.2 F g^{-1} at 10 mV s^{-1} with a high specific energy of 44.6 Wh kg^{-1} at a high specific power of 2889.9 W kg^{-1} and better cycling stability with ≈90% retention of the initial capacitance after 10000 cycles.

Polythiophene-based composite electrodes have also been developed and employed for SCs. Nanocomposite electrode materials **P67**-g-GO, containing GO and polythiophene with OEG side chain (**P67**), were synthesized by covalently grafting **P67**, prepared by in situ oxidative chemical polymerization, to GO nanosheets through an esterification reaction (**Scheme 4**).[144] The **P67**-g-GO electrode displayed a quasi-rectangular CV curve which indicated the pseudocapacitive contribution of **P67** and attained an improved performance with a maximum C_s of 971 F g^{-1} at 1 A g^{-1} in a half cell which is higher than that of GO, **P67**, and the physical blend of GO and **P67**. The nanocomposite showed high cyclic stability with retention of 98% of its initial capacitance after 1 000 0 cycles. A solid-state type I device fabricated from **P67**-g-GO exhibited C_s of 403, 842, and 191 F g^{-1} at 1.25 A g^{-1} for single devices, two devices in parallel, and two devices in series, respectively. **P68**-g-SWCNT with poly(3-oligo(ethylene oxide))thiophene (**P68**), covalently grafted onto the surface of SWCNT via OEG linkages, was also reported.[145] **P68**-g-SWCNT attained a C_s of 399 F g^{-1} at 1 A g^{-1} with over 91% capacitance retention after 8000 cycles but lower than the **P67**-g-GO electrode. These studies indicate that OEG side chain not only links the polymer with 2D materials covalently but also greatly improves the charge transfer and ionic transport.

Hu et al.[146] prepared PDAAQ/CGO electrode by anchoring 1,5-diaminoanthraquinone (DAAQ) on the surface of cetyltrimethylammonium bromide-modified GO (CGO), and directional growth of poly(1,5-diaminoanthraquinone) (PDAAQ) by in situ chemical polymerization. The PDAAQ/CGO electrode material gave a high C_s of 760 F g^{-1} at 1 A g^{-1} and good cycling

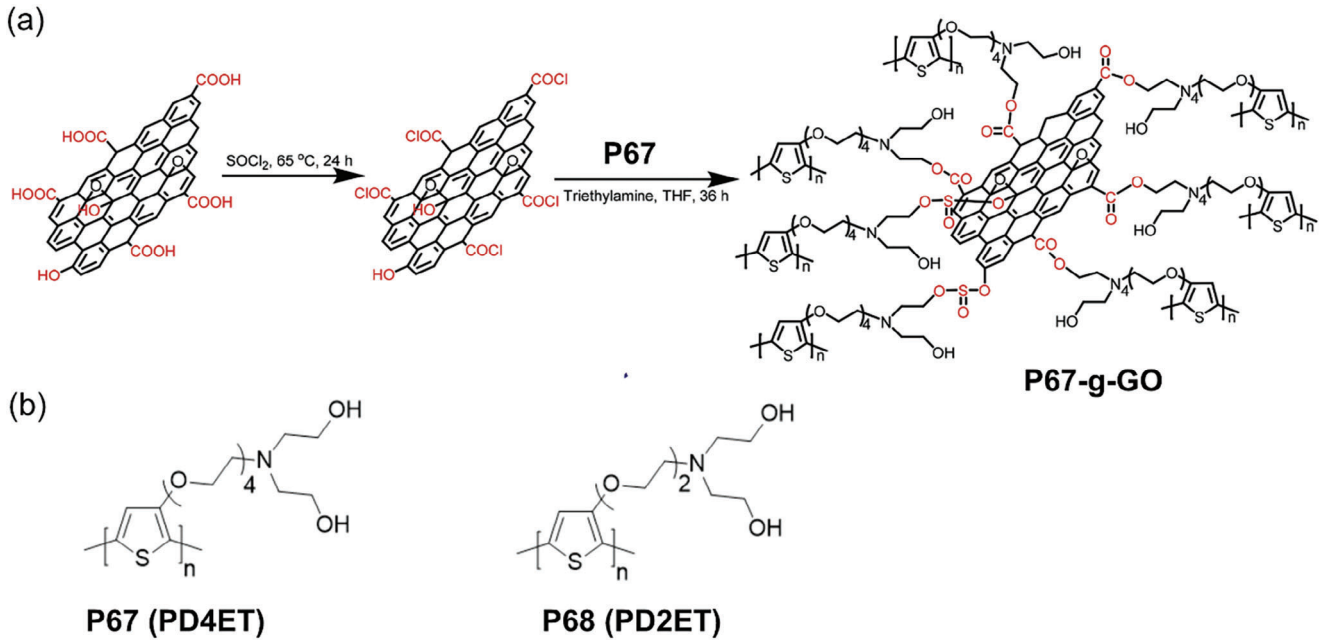

Scheme 4. Schematic illustration for the covalent grafting of **P67** side chains to GO a) and structures of **P67** and **P68** b). (adapted from Ref. [144])

stability (90.4% after 10000 cycles) in a half cell. Electrochemical kinetic study showed that the majority of the capacity of PDAAQ/CGO electrodes originates from the surface capacitive effect. The asymmetric SCs, fabricated using PDAAQ/CGO as a negative electrode and nitrogen-doped carbon (obtained by carbonizing pure PDAAQ) as a positive electrode, attained a C_s of 74 F g^{-1} at 1 A g^{-1}, an E_D of 41.1 Wh kg^{-1} at a P_D of 1000 W kg^{-1} and a cyclic stability of 83% after 10000 cycles.

Recently, composite materials based on the n-type polymer **P51** (Figure 10) and MWCNT, synthesized by modified in situ Stille polymerization were reported.[147] The **P51**/MWCNT composite material exhibited a battery-type electrochemical behavior and a specific capacity of 80 mAh g^{-1} in a half cell using 1M $LiClO_4$/propylene carbonate as an electrolyte, which is higher than the pristine **P51** and physically mixed **P51**/MWCNT composite. A high-voltage (2.4 V) hybrid SC consisting of **P51**/MWCNT as a negative electrode and activated carbon as a positive electrode with 1M $LiClO_4$/propylene carbonate delivered a specific capacity of 8.5 mAh g^{-1} at 0.2 A g^{-1}.

Polyindole/MWCNT (**P11**/MWCNT) composite electrode was also synthesized by an in situ chemical oxidative polymerization of indole monomer with MWCNT.[148] The PIN/MWCNT electrode attained a maximum C_s of 555.6 F g^{-1} (half-cell) at 0.5 A g^{-1} in a nonaqueous system with a retention of 91.3% after 5000 cycles, which is higher than the pristine polyindole.

Besides CNT, graphene has also been used in the polymer composite fabrication. For example, a porous nanocomposite (GNS/a-MWCNT/PDAAQ) prepared by in situ chemical oxidative polymerization of PDAAQ on graphene nanosheets/acid-treated MWCNT was also reported.[149] The electrode showed pseudocapacitance characteristics in a broader potential window (−2 to 0.8 V) and achieved C_s up to 274 F g^{-1} in the negative and 137 F g^{-1} in the positive region. When the composite electrode was assembled into a symmetric SC, the device showed an output voltage of 2.8 V, a maximum E_D of 86.4 Wh kg^{-1} at P_D of 0.73 kW kg^{-1}, good rate performance and cycling stability with only 7% capacitance loss after 10 000 cycles.

3.4.2. Polymer Composites with MXene

In situ polymerization has been considered a straightforward strategy to form composite materials from polymers and 2D transition metal carbides, nitrides, and carbonitrides (MXenes). In the MXene-polymer composites, the presence of polymers serves to enhance the interlayer spacing of MXene, thereby facilitating the establishment of a greater number of electron-ion channels and interaction sites. Consequently, these enhancements contribute significantly to the overall performance improvement of the composites.[150,151] For instance, Gogotsi et al.[152] developed PPy/MXene by oxidant-free in situ polymerization of PPy in between $Ti_3C_2T_x$ layers (T is a surface terminating functionality such as O, OH, and/or F and x is the number of terminating groups). PPy/MXene showed pseudocapacitive behavior and gave a high C_s of 416 F g^{-1} (1000 F cm^{-3}) at 5 mV s^{-1} and excellent cyclic stability up to 25000 cycles with 92% capacitance retention (half-cell). The high capacitance and cyclic stability were ascribed to the microarchitecture of PPy/MXene in which the aligned PPy in between $Ti_3C_2T_x$ layers gave rise to high conductivity, fast and reversible redox reactions, and short diffusion length.

MXene/PPy-PVA hydrogel synthesized by in situ polymerization of pyrrole absorbed into the MXene-PVA hydrogel network was also reported.[153] The MXene/PPy-PVA hydrogel attained a higher capacitance of 614 F g^{-1} (at 1 A g^{-1}) than that of MXene hydrogel and remarkable cycling stability with 100% capacitance retention over 10000 cycles (half-cell). A solid-state symmetric SC with MXene/PPy-PVA hydrogel electrodes and H_2SO_4/PVA gel electrolyte exhibited a C_s of 184 F g^{-1} with an E_D of 30.9 Wh kg^{-1}

and a P_D of 605 W kg^{-1} at a discharge rate of 1 A g^{-1}. Moreover, Guo et al.[154] reported a highly conductive textile electrode PPy/MXene/PMFF for SC prepared by in situ chemical polymerization of PPy on MXene/polyethyleneimine-modified fiber fabric (PMFF). The electrode showed a quasi-rectangular shaped CV curve and a symmetric GCD curve, both in half cell and device, which indicate that charge storage is dominated by pseudocapacitive behavior. As a result of excellent interfacial engineering between PPy and MXene/PMFF, PPy/MXene/PMFF delivered a high C_s of 439 F g^{-1} (1295 mF cm^{-2}), excellent cycling stability with 94.8% retention after 30000 cycles and mechanical properties with no degradation of electrochemical performance upon deformations (half-cell). A solid-state symmetric SC assembled with the PPy/MXene/PMFF also gave a high areal capacitance of 458 mF cm^{-2} at 1 mA cm^{-2} and showed a maximum E_D of 40.7 μWh cm^{-2} and a P_D of 25 mW cm^{-2} with high cycling stability (with only 6.3% capacitance deterioration after 30000 cycles).

In addition to PPy, PANI and polyindole have been integrated with MXene to manufacture composite electrodes for SCs. Freestanding PANI/MXene films with various thicknesses were made by in situ polymerization of PANI on MXene sheets and were systematically investigated.[155] The MXene/PANI electrodes delivered enhanced C_s as high as 503 F g^{-1} (1682 F cm^{-3}) at 2 mV s^{-1}, and after 10000 cycles retained 98.3% of their capacitance in a three-electrode system. Astonishingly, the electrode with a high thickness (90 μm) and mass loading (23.82 mg cm^{-2}) gave a high C_s of ≈336 F g^{-1} (888 F cm^{-3}).

Recently, Nayak et al.[156] prepared pseudocapacitive polyindole (**P11**)/MXene (3:1 ratio) nanocomposite and fabricated both symmetric and asymmetric devices. The symmetric device afforded a C_s of 226.5 F g^{-1} at 2 A g^{-1} and retained 90.5% of its capacitance after 8000 cycles. Furthermore, the asymmetric device with **P11**/MXene as an anode gave a maximum C_s of 117 F g^{-1} and an E_D of 65.3 Wh kg^{-1} and retained 88% of its capacitance after 6000 cycles. The high performance is attributed to the synergistic effect of each pseudocapacitive component and the improved surface area and porosity of the composite.

3.4.3. Polymer Composites with Biomolecules and Biopolymers

In situ polymerization has also been found to be a promising method for preparing biomolecule- and biopolymer-based composite electrodes for energy storage.[157] Shen and co-workers[158] demonstrated free-standing electrodes containing bacterial cellulose (BC) for flexible SCs. The BC/MWCNT/PANI composite electrode was made by depositing multi-walled carbon nanotubes on BC paper followed by in situ polymerization of aniline on BC-MWCNT. The flexible electrode showed a high C_s of 656 F g^{-1} at 1 A g^{-1} in a half cell with 99.8% retention after 1000 cycles. An all-solid symmetric (type I) SC showed good mechanical flexibility due to highly flexible BC and strong bonding between the MWCNT and BC.

Cheng et al.[39] further improved the C_s of PANI/BC-based composite electrodes by combining nickel-cobalt layered double hydroxide (NiCo-LDH) with PANI/BC through in situ chemical polymerization and chemical bath deposition method. Benefiting from the synergetic effect, the flexible NiCo-LDH/PANI/BC electrode delivered a high C_s of 1690 F g^{-1} at 1 A g^{-1} in a half cell with high rate capability (778 F g^{-1} at 15 A g^{-1}) and high cycling stability (83.2% retention after 5000 cycles). The CV and GCD clearly indicate a battery-type behavior although the authors claim it has a pseudocapacitive behavior.[159] The electrode also exhibited high tensile strength and electrochemical stability during bending and stretching. Moreover, a flexible all-solid-state asymmetric SC, with NiCo-LDH/PANI/BC as a positive electrode and N-doped carbonized BC/carbon cloth (N-CBC/CC) as a negative electrode, showed a maximum C_s of 133.1 F g^{-1} with an E_D of 47.3 Wh kg^{-1} at a P_D of 828.9 W kg^{-1} and a moderate cycling stability (91.4% capacitance retention after 3000 cycles).

Chemically bonded ternary composites, PPy/BC/GO, prepared by coating PPy via in situ chemical polymerization of pyrrole on BC/GO binary composite, were reported.[160] It was found that the restacking of graphene layers and aggregation of BC fibers was prevented due to the complementary bond between BC and GO. PPy/BC/GO showed pseudocapacitive characteristics, high electrical conductivity (1320 S m^{-1}), and volumetric capacitance (278 F cm^{-3}) along with a high C_s of 556 F g^{-1} for a half cell with 95.2% capacitive retention after 5000 cycles. Notably, the composite delivered a high C_s of 486 F g^{-1} with 93.5% retention after 2000 cycles in symmetric SCs.

Besides, polymerization on nanocellulose, such as cellulose nanofibrils (CNFs), can also inhibit agglomeration and enhance the conductivity, electrochemical and mechanical performances of the SCs.[161] Aerogel electrode materials CNF/VGCF/PPy with higher conductivity, made by in situ polymerization of PPy on CNF/ vapor grown carbon fiber (VGCF) hybrid aerogels, were reported by Wang et al.[162] The CNF/VGCF aerogels resulted in a porous network structure, which is good for absorbing more electrolytes and providing more sites for redox reactions. The pseudocapacitive aerogel electrode gave a high C_s of 850.27 F g^{-1} at 3.125 mA cm^{-2} in a half cell. Interestingly, the all-solid-state SC device based on CNF/VGCF/PPy afforded a high C_s of 678.66 F g^{-1} at 1.875 mA cm^{-2} and maintained 91.38% of its initial capacitance after 2000 cycles.

It was rationalized that the charge storage capacitance of conjugated polymers can be increased by combining them with redox-active organic materials that contain functional groups such as phenol, and quinones. The capacitance improvement is attributed to the oxidation and reduction of the functional groups via the formation of redox-active quinone/hydroquinone (Q/QH2) structures in the biopolymer and doped in the polymer matrix.[163,164] These functional groups are found in biomolecules such as lignin,[165] juglone[166] and tannin.[167] Lignin (LG) biopolymer has plenty of phenol groups that can be oxidized to quinone groups and used as redox components in energy storage.[168] The composites of lignin and polymers have been widely used as electrode materials for cost-effective and bio-inspired energy storage devices.[169,170]

More stable sulfonated lignin and PEDOT biocomposite (LG/PEDOT) was synthesized using in situ chemical polymerization and electrochemical polymerization by Ajjan et al. (**Scheme 5**).[171] The chemically polymerized LG/PEDOT electrode gave a lower C_s of 115 F g^{-1}, while the electrochemically polymerized one gave a C_s of 170.4 F g^{-1}, which is more than twice that of PEDOT (80.4 F g^{-1}) due to additional pseudocapacitance produced by the quinone units in LG. As compared to LG/PPy, LG/PEDOT was more stable with 83% capacitance

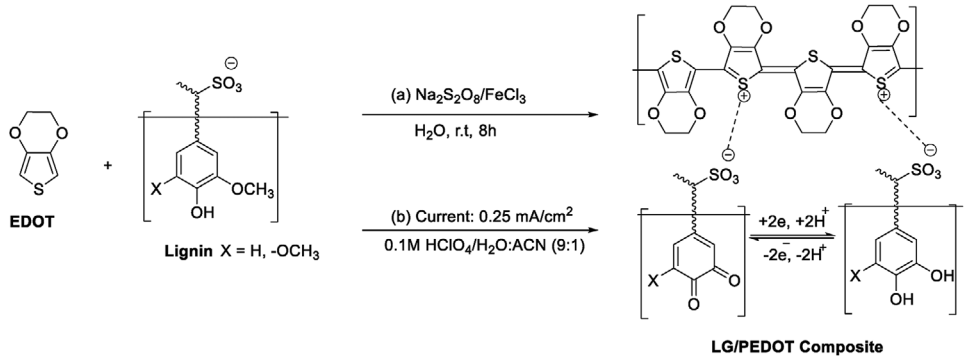

Scheme 5. In situ chemical oxidative polymerization (path a) and in situ electrochemical polymerization (path b) of LG/PEDOT composite (adapted from Ref. [171]).

retention after 1000 cycles. Berggren et al.[172] further improved the C_s of PEDOT to 230 F g^{-1} by adding LG into a composite material of cellulose nanofibrils and PEDOT:PSS, which indicates that LG is compatible with polymers and paper-based SCs.

Inganäs et al.[163] developed a ternary composite (PPy/HMA/LG) electrode containing PPy, LG, and phosphomolybdic acid (HMA) by simple, one-step, in situ polymerization. The C_s of the binary composite PPy/LG were improved from 477 to 682 F g^{-1} at 1 A g^{-1} (half-cell) by adding HMA and the charge storage capacity improved significantly from 69 to 128 mAh g^{-1} as a result of the synergistic effect (the contributions of redox reaction) of HMA and LG in the ternary composite.

Lignin/polymer composites made by in situ polymerizations have also been used for flexible SCs. Wu and Zhong[173] developed a freestanding conductive electrode LG/PANI/FGH/FCC by grafting functionalized graphene hydrogel (FGH) in oxidized carbon cloth followed by deposition of LG/PANI hydrogel via in situ chemical polymerization of aniline in the presence of LG. The LG/PANI/FGH/FCC-based symmetric SC displayed pseudocapacitive behavior and areal capacitance of 1223 mF cm^{-2} and an E_D of 169.9 mWh cm^{-2} at a P_D of 1000 mW cm^{-2} using 1M H_2SO_4 electrolyte. The flexible all-solid-state SC based on LG/PANI/FGH/FCC with H_2SO_4/polyvinylalcohol (PVA) gel electrolyte exhibited a specific areal capacitance of 1156 mF cm^{-2} with excellent flexibility. The lower capacitance was ascribed to slow ion diffusion in the SC in the H_2SO_4/PVA gel electrolyte than the SC in the 1 M H_2SO_4 electrolyte.

Overall, in situ polymerization serves as an efficient design tool for fabricating binder-free and flexible nanostructured composite electrode materials based on polymers. Half-cell and symmetric SCs constructed from these composites have demonstrated C_s up to 1700 F g^{-1} and 1335 F g^{-1}, respectively.[39–41] Moreover, this method holds promise for combining conjugated polymers with abundant biopolymers, contributing to the development of green and sustainable energy storage devices. However, it is important to note that this polymerization method may not be environmentally friendly, as it often involves the use of non-renewable and toxic solvents to incorporate other materials into the polymer matrix. Thus, to make this technique more eco-friendly and sustainable, green solvent-processable polymers with water-solubilizing groups need to be carefully designed to blend with the biopolymers through in situ polymerization under aqueous or other green solvent conditions.[174]

In general, the three polymerization methods discussed above have been widely employed to prepare both p-type and n-type polymer-based electrode materials for SCs. Each technique has its own set of advantages and disadvantages, which are summarized in **Table 1**.

4. Electrolytes for Polymer-Based Pseudocapacitors

Besides electrode materials and device configuration, the capacitance, energy density, and stability of SCs are significantly influenced by the electrolyte composition. In this section, we provide a comprehensive overview of the commonly used electrolytes and the key criteria for their selection. For a more extensive exploration, readers are encouraged to refer to other review articles that specifically focus on electrolytes for energy storage applications.[175,176]

The electrolytes used in SCs can be classified as aqueous, organic, and ionic liquids. There are two main criteria that electrolytes should fulfill for application in efficient SCs: 1) The electrolyte should have a wider, electrochemically stable, potential window than that of the electrode materials to maximize the energy density of the device. The aqueous electrolyte (acidic, alkaline, and neutral)–based SCs work in the potential window of 1.0 to 1.3 V limited by the electrolysis of water. On the other hand, the organic and ionic liquid electrolyte-based SCs generally work at higher potential windows of 2.0–2.7 and 3.5–4.0 V, respectively, which result in higher energy density and power density than the aqueous devices. 2) The electrolyte should have high ionic conductivity.[175] In this regard, aqueous electrolytes have higher conductivity (up to 1 S cm^{-1}) as compared to organic and ionic liquid electrolytes, which is valuable for lowering the equivalent series resistance (ESR) and maximizing the power density of the aqueous-based SCs.[177]

Owing to the development of flexible SCs, polymer electrolytes received more attention. Gel polymer electrolytes have been dominantly used for the fabrication of all-solid and flexible SCs due to their advantages such as high ionic conductivity, tunable characteristics, and bendable structures for diverse applications.[178,179] Several polymers have been employed for making gel polymer electrolytes like poly(acrylic acid) (PAA), poly(vinyl alcohol) (PVA), poly(ethylene oxide) (PEO), potassium polyacrylate (PAAK), poly(ether ether ketone) (PEEK), poly(methyl methacrylate) (PMMA), and poly(vinylidene

Table 1. Comparison of the polymerization methods.

Polymerization methods	Advantages	Disadvantages
Electropolymerization	• One-step process for both synthesis and coating • Electrodes can be directly used for SCs. • Obtained polymer electrodes are highly porous with high surface area.	• Monomers with high oxidation potential cannot be polymerized. • Challenge in their determination of the molecular weight of polymer • Reproducibility issue for polymers with consistent redox and structural properties poses difficulties. • Difficulty in achieving high loading due to self-limiting growth process • Challenge in the Preparation of nanostructured composite electrodes.
Chemical polymerization	• Allows preparation of D-A polymers with various donor and acceptor units • Suitable for mass production • Suitable for solution-processable *p*-type and *n*-type polymers	• Not atom economical and eco-friendly, • toxic transmetallating reagents are needed. • Increased synthetic steps and cost • Low capacitance and energy density.
in situ polymerization	• Low cost • Short reaction time • Suitable for nanostructured composite electrodes • Appropriate for large-scale production • Efficient combination of conjugated polymers with biopolymers	• Not environmentally friendly, nonrenewable and toxic solvents are used.

fluoride-*co*-hexafluoropropylene) (PVDF-HFP).[175] In general, for high-performance, flexible, and all-polymer SCs, polymer electrolytes that are compatible with the electrodes need to be carefully designed with the help of molecular simulation techniques and prepared at low cost and through the use of efficient methods.

5. The Stability of Polymer-Based Pseudocapacitors

Besides improving the performances of the SC devices, improving the cyclability and electrochemical stability of pseudocapacitors is essential for real-world applications. Most of the SC devices based on polymers maintained 80%–100% of the initial capacitance after 5000–12 500 cycles (**Table 2**). The longevity of polymer-based SC devices is mainly diminished by, i) the collapse of the polymer structure (structural disintegration) due to swelling and shrinking (volumetric change) caused by the flow of ions in and out of the polymer matrix during charging/discharging,[25,60,80] ii) overoxidation of the polymers by charging to potentials greater than their operating potential windows may irreversibly damage their electrochemical activities. Further, the electrochemical stabilities of the electrolytes also influence the stabilities of the devices.

Thus, different strategies have been employed to overcome the above-mentioned limiting factors that affect the stability of polymer-based pseudocapacitors. For example, Heeger and coworkers[181] developed a method to improve the stability of PANI-based SCs by combining PANI as the porous electrochemically-active material and benzoquinone-hydroquinone (BQHQ) redox couple as an electrolyte. The quinone in the PANI-quinone SC forms a tunable redox shuttle that controls the electron transfer process at the PANI-modified electrodes and reduces the level of unfavorable redox processes in PANI. As a result, the SCs present high pseudocapacitance and superb cycling stability with no capacitance degradation after 50000 cycles compared to pure PANI-based SC devices.

Developing porous networks through the formation of composites of polymers with carbon materials has been used to improve the stability of SC devices.[182,183] Xu et al.[184] demonstrated 85% capacitance retention after 60000 cycles for electropolymerized ultrathin PANI nanolayers on the surface of graphene sheets. It was found that the nanolayers reduced the volumetric change by giving a space buffer for the expansion of the polymer without affecting the entire structure of the composite. The volume change during doping/dedoping has been suppressed by developing a PANI-based hybrid hydrogel network which maintained 92% of the initial capacitance after 35000 cycles.[185]

The higher molecular order of a polymer can also increase the cycling stability of SCs. Supercapacitors based on electropolymerized PPy that retained more than 97%, 91%, 86%, and 50% capacitance after 15 000, 50 000, 100 000, and 230 000 charging/discharging cycles, respectively, were reported by Zhi and co-workers.[186] The high stability is mainly ascribed to the molecular ordering created with the aid of an electric field that favors a homogeneous stress distribution and charge transfer. It was inferred that tuning the structure of the polymer and selecting appropriate electrolytes can also improve the stability of the device. Reynolds et al.[187] investigated the stability of SCs as a function of electrolytes using PEDOT and ProDOT as electrode couples. The type I SC based on PEDOT and ProDOT showed high cycling stability with retention of 98% of the initial capacitance throughout 50 000 charge/discharge cycles in the ionic liquid electrolyte 1-ethyl-3-methyl-1*H*-imidazolium bis(trifluoromethanesulfonyl)imide (EMI-BTI). Electrochemically stable type I SCs with poly(2,2-dimethyl-3,4-propylenedioxy-thiophene) (PProDOT-Me2) as pseudocapacitive material and EMI-BTI as an electrolyte, which maintained 85% of the initial capacitance over 32000 cycles, were reported by Liu and Reynolds.[188] Likewise, Reynolds et al.[69] demonstrated that

Table 2. Summary of the characteristics of polymer-based SCs.

Polymers and composite	Type of device	Mass C_s [F g^{-1}]	Area C_s [mF cm^{-2}]	Mass loading	Volume C_s [F cm^{-3}]	Electrolyte	C_s Retention, cycles	Synthesis method	Refs.
PANI	Half cell	950 at 1 A g^{-1}	–	–	–	1 M H_2SO_4	93%, 500	EP	[63]
P6	Half cell	82.2 at 0.1 mA cm^{-2}	41.1 at 0.1 mA cm^{-2}	–	164.4 at 0.1 mA cm^{-2}	1 M $LiClO_4$		EP	[75]
	ASSC	32.9 at 0.1 mA cm^{-2}	–	–	–	PMMA : $LiClO_4$	86%, 7000	EP	[75]
P8	Type I	640 at 1 mA cm^{-2}	–	–	–	PMMA : $LiClO_4$	92.5%, 10000	EP	[76]
P14	Half cell	416 at 10 A g^{-1}	–	–	–	1 M H_2SO_4	83%, 5000	EP	[86]
P22	Half cell	149 at 10 mV s^{-1}	151.2 1 mA cm^{-2}	–	–	0.1 M $TBAPF_6$/ACN	100%, 2000	EP	[95]
P23	Half cell	92 at 1 A g^{-1}	–	–	–	MeCN–Bu_4NBF_4	90%, 1000	EP	[96]
P27	Half cell	299 at 5 A g^{-1}	–	–	271 at 5 A cm^{-3}	0.1 M Bu_4NPF_6	–	EP	[99]
P29	Type III	78.6 at 0.5 A g^{-1}	–	–	–	0.1 M Bu_4NPF_6	80%, 1000	EP	[100]
PANI and graphene	Half cell	763 at 1 A g^{-1}	–	–	–	1 M H_2SO_4	82%, 1000	in situ EP	[138]
Pg^{-1}	Half cell	791 at 1.14 A g^{-1}	8863 at 12.7 mA cm^{-2}	11.2 mg cm^{-2}	–	1 M H_2SO_4	81.1%, 10000	in situ EP	[139]
	Type I	712 at 1.08 A g^{-1}	–	>10 mg cm^{-2}	–	1 M H_2SO_4	–	in situ EP	[139]
PANI–Toray paper	Half cell	1700 at 5 mV s^{-1}	–	–		0.5 M H_2SO_4	–	in situ EP	[41]
	Type I	1335 at 10 A g^{-1}	1300 at 10 A g^{-1}	–		PVA/ H_2SO_4 gel	85%, 10000	in situ EP	[41]
MoS_2@PANI	– Type I	853 at 1 A g^{-1}	–	–	–	0.5 M H_2SO_4	91%, 4000	in situ EP	[140]
MoS_2/PPy/PANI	Half cell	1273 at 0.5 A g^{-1}	–	–	–	0.5 M H_2SO_4	83%, 3000	in situ CP	[142]
PGF	Type I	1124 at 0.25 A g^{-1}	–	–	–	1 M H_2SO_4	82%, 10000	in situ CP	[40]
r–PGMGN	Type I	882.2 at 10 mV s^{-1}	–	0.25 mg /cm^{-2}	–	1 M KCl	~90%, 10000	in situ CP	[143]
P67–g–GO	Half cell	971 at 1 A g^{-1}	–	–	–	1 M KOH	98%, 10000	CP	[144]
	Type I	403 at 1.25 A g^{-1}	–	–	–	1 M KOH	–	CP	[144]
PDAAQ/CGO	Half cell	760 at 1 A g^{-1}	–	–	–	1 M H_2SO_4	90.4%, 10000	in situ CP	[146]
	ASSC	74 at 1 A g^{-1}	–	–	–	1 M H_2SO_4	83%, 10000	in situ CP	[146]
PIN/MWCNT	Half cell	555.6 at 0.5 A g^{-1}	–	0.4 g cm^{-3}	222.2 at 0.5 A g^{-1}	1 M LiPF6	91.3%, 5000	in situ CP	[148]
CNF/VGCF/PPy	Half cell	850.27 at 3.125 mA cm^{-2}	–	–	–	1 M H_2SO_4	–	in situ CP	[162]
		678.66 at 1.875 mA cm^{-2}	8.61 at 1 mV s^{-1}			PVA/H_3PO_4 gel	91.38%, 2000	in situ CP	[162]
BC/MWCNT/ PANI	Half cell	656 at 1 A g^{-1}	–	–	–	1 M H_2SO_4	99.8%, 1000	in situ EP	[158]
PPy/BC/GO	Half cell	556 at 0.4 A g^{-1}	–	–	278	1 M H_2SO_4	95.2%, 5000	in situ CP	[160]
	Type I	486 at 0.63 A g^{-1}	–	1.6 mg	243	1 M H_2SO_4	93.5%, 2000	in situ CP	[160]
NiCo–LDH/ PANI/BC	Half cell	1690 at 1 A g^{-1}	–	–	–	2 M KOH	83.2%, 5000	in situ CP	[39]
	ASSC	133.1 at 1 A g^{-1}	–	–	–	2 M KOH	91.4%, 3000	in situ CP	[39]
PPy/HMA/LG	Half cell	682 at 1 A g^{-1}	–	49.6 μg cm^{-2}		0.1 M HNO_3	–	in situ EP	[163]
PPy/MXene	Half cell	416 at 5 mV s^{-1}		0.93 mg cm^{-2}	1000 at 5 mV s^{-1}	1 M H_2SO_4	92%, 25000	in situ CP	[152]

(*Continued*)

Table 2. (Continued)

Polymers and composite	Type of device	Mass C_s [F g^{-1}]	Area C_s [mF cm^{-2}]	Mass loading	Volume C_s [F cm^{-3}]	Electrolyte	C_s Retention, cycles	Synthesis method	Refs.
MXene/PPy–PVA	Half cell	614 at 1 A g^{-1}	–	0.049 mg cm^{-2}	425 at 2 mA cm^{-3}	1 M H_2SO_4	100%, 10000	in situ CP	[153]
	SSC	184 at 1 A g^{-1}	–	0.049 mg cm^{-2}	–	PVA/ H_2SO_4 gel	83%, 1000	in situ CP	[153]
PPy/MXene/PMFF	Half cell	439 at 1 mA cm^{-2}	1295 at 1 mA cm^{-2}	–	–	1 M H_2SO_4	94.8%, 30000	in situ CP	[154]
	Type I		458 at 1 mA cm^{-2}	–	–	PVA/Na_2SO_4 gel	93.7%, 30000	in situ CP	[154]
MXene/PANI	Half cell	503 at 2 mV s^{-1}	–	–	1682 at 2 mV s^{-1}	3 M H_2SO_4	98.3%, 10000	in situ CP	[155]
P11/MXene	Type I	226.5 at 2 A g^{-1}	–	–	–	1 M $TEABF_4$ /DMSO	90.5%, 8000	in situ CP	[156]
	ASSC	117 at 1 A g^{-1}	–	–	–	1 M $TEABF_4$ /DMSO	88%, 6000	in situ CP	[156]
PANI/rGO	Half cell	824 at 2.22 A g^{-1}	–	7.1 mg cm^{-2}	–	0.5 M H_2SO_4	–	CP	[102]
P30/ SWNT	Half cell	112.4 at 1 A g^{-1}	–	0.04 mg cm^{-2}	–	0.1 M $LiClO_4$	82%,12500	CP	[103]
P32	Type I	31.5 at 50 mV s^{-1}	–	170 µg cm^{-2}	–	0.5 M LiBTI–PC	82%, 50000	CP	[104]
P40	Half cell	319 at 0.2 mA cm^{-2}	64.8 at 0.2 mA/cm^2	0.3 mg cm^{-2}	–	1 M H_2SO_4	83%, 1000	CP	[107]
MWCNT–**P45**	Half cell	175 at 0.5 mA cm^{-2}	17.5 at 0.5 mA cm^{-2}	0.1 mg cm^{-2}	–	0.5 M $LiClO_4$/PC	95.1%, 5000	CP	[109]
	SSC	54.6 at 0.2 mA cm^{-2}	5.46 at 0.2 mA cm^{-2}	–	–	$LiClO_4$/PC–PMMA	96%, 5000	CP	[109]
P53	Type III	124 at 0.5 A g^{-1}	–	–	–	0.5 M H_2SO_4	100%, 5000	CP	[118]
P56	Half cell	113 at 0.5 A g^{-1}	–	–	–	1 M PC–$LiClO_4$	100%, 4000	CP	[119]
P60	Type IV	33 at 1 A g^{-1}	90	2–5 mg	–	0.4 M Na_2SO_4	100%, 10000	CP	[125]
P61	Half cell	245 at 5 mV s^{-1}	–	–	–	1 M H_2SO_4	36.7%, 5000	CP	[126]
P61/rGO	Half cell	659 at 1 A g^{-1}	–	–	–	1 M H_2SO_4	–	CP	[126]
	ASSC	125 at 1 A g^{-1}		–	–	1 M H_2SO_4	71.8%, 10000	CP	[126]
P66	Half cell	689 at 0.5 A g^{-1}	–	6.4 mg cm^{-2}	–	6 M KOH	92%, 50000	CP	[42]
PProDOT–Me2	Type I	55 at 0.3 mA cm^{-1}	–	60 µg cm^{-2}	–	EMI–BTI	85%, 32000	EP	[188]

Abbreviations: CP: Chemical polymerization. The classification of the devices as type I, II, III and IV is described in section 2 and Figure 2.

80% of the initial capacitance was retained after 400 000 cycles for flexible, type I PEDOT-based SCs in EMI-BTI electrolyte due to lower volume changes in the oxidized state that resulted in less mechanical stress.

The characteristics of high-performance polymer-based electrode materials and their synthesis methods are summarized in Table 2. The mass loading and type of devices, as well as the electrolyte, need to be considered for a fair comparison of the performance of the materials.

n-Type and ambipolar polymer electrodes suffer severe cyclic instability caused by the charge trapping (CT) effect during the n-doping process. One strategy to suppress the CT effect is optimizing the morphology to facilitate fast electron transport and rapid ion diffusion. Recently, Ma et al.[189] demonstrated that **P24**, obtained by depositing 2,6-bis(3-methyl-9*H*-carbazol-9-yl)anthracene-9,10-dione on vertically standing graphene (VSG) by electropolymerization, achieved better morphology which shortened the charge transfer distance and reduced the CT effect. Thus, the **P24**/VSG-based SC retained 88% of the capacitance after 10000 cycles, which is more stable than the polymer without VSG.[97]

The abovementioned methods used for enhancing stability may not work for all types of polymer pseudocapacitors and thus need further investigation. In general, cycling stability studies suggest a bright future for the molecular design of stable and scalable SCs with commercial operating lifetimes.[190]

6. Conclusion and Outlook

Conjugated polymers are very promising materials for future high energy density SC applications owing to their tunable conductivity, good processability, low cost, lightweight, flexibility, controllable resistance over a wide range, and excellent

electrochemical properties. In this review, the synthesis of polymers by electropolymerization, in situ polymerization, and chemical polymerization methods and their performances in SCs have been summarized. The electropolymerization methods have been used for making polymer electrode materials with stable morphology, high porosity, and surface area. Electropolymerization also improves molecular ordering and facilitates uniform stress distribution and charge transfer which results in high cyclic stability. However, suitable monomers for electropolymerization are very limited and the method is not suitable for large-scale production of solution-processable polymers. The in situ polymerization technique is an efficient method to develop polymer-based nanostructured composite materials by combining them with other materials like graphene and easily available biopolymers, which give large surface area, short charge transport paths, and better electrochemical and mechanical properties over pure polymers. However, it is difficult to control the morphology and component distribution of the polymers in the composite materials by this method.

On the other hand, chemical polymerization has been used to prepare several solution-processable n-type and p-type polymers by combining different donor and acceptor monomeric units. These polymers are also very promising for the fabrication of flexible electrochromic SCs. However, most of these polymers show low C_s and energy density as compared with the state-of-the-art composite electrode materials. The complexity of synthesis, high cost, and use of toxic metals like those used in the Stille polymerization, limit the chemical polymerization technique for sustainable applications.

The ideal polymeric electrode materials for high-performance SCs must possess high porosity, large surface area, high charge mobility, fast ion transport, and stable morphology across a wide potential range. Among the homopolymers, PANI-based materials have demonstrated exceptional specific capacitance of up to 1700 F g^{-1} in half cells and 1335 F g^{-1} in symmetric SCs, accompanied by an energy density of 30 Wh kg^{-1} and power density of 2000 W kg^{-1}, while exhibiting impressive capacitance retention of over 80% after 10 000 cycles. Composite materials combining polymers with graphene, MXene, and cellulose have exhibited remarkable performance, with the PPy/MXene composites in particular showcasing high specific capacitance of up to 614 F g^{-1} and exceptional cyclic stability, retaining up to 95% of their capacitance after 30000 cycles.

The majority of polymers and their composites exhibit electrochromic properties and demonstrate superior performance in flexible electrochromic SC devices. The incorporation of EDOT and its derivatives into the D-A-type polymer backbone has led to the development of high-performance electrochromic p-type and ambipolar polymers. Furthermore, n-type polymers incorporating NDI and PDI as acceptor units have exhibited highly promising performances. Specifically, PDI-based polymers have showcased a high specific capacitance of up to 689 F g^{-1} with excellent cycling stability of up to 50 000 cycles in half cells, and a specific capacitance of up to 125 F g^{-1} in asymmetric devices.

The substitution of alkyl side chains in polymers with hydrophilic polar side chains has been found to facilitate ion transport and enhance the compatibility of SCs with aqueous electrolytes. In general, polymer-based SC devices have achieved elevated cell voltages (up to 4.8 V for p-type polymers and 3 V for n-type polymers) and exceptional cyclic stability, with over 80% retention of capacitance after 100000 cycles. Consequently, future research should prioritize increasing capacitance and advancing the mechanical robustness of polymer-based SCs, while maintaining high voltage levels and stability.

Despite significant progress in the preparation of many conjugated polymers using different techniques, their capacitance still falls below the theoretically expected values, and the energy densities of SC devices remain low, thereby restricting their large-scale applications. The low conductivity of pure polymers and lack of stable n-type polymers are also the current challenges facing the efforts to boost the performance of polymer-based SC devices. These properties depend not only on polymerization methods but also on the structures of polymers and the composite materials and device architectures. Future possible strategies for improving the intrinsic properties of the electrode materials shall consider:

6.1. Improving the Conductivity of Polymers

The low conductivity of polymers and/or electrode materials causes large ESR and joule heating of the electrodes during the charging/discharging cycle, which diminishes the charging efficiency, energy density, and power density.[191] Combining polymers with highly conductive 2D materials such as graphene and MXene, either through in situ polymerization or physical blending, represents an efficient approach to achieving high-conductivity electrode materials. This enables fast and reversible redox reactions and shorter ion diffusion lengths. Additionally, by avoiding binders that hinder device conductivity and instead focusing on the development of polymer electrodes via electropolymerization and self-standing materials, it becomes possible to significantly enhance the performance of SCs.

6.2. Minimizing the Swelling and Shrinking of The Polymers

The long-term stability of the polymer-based SCs is largely limited by the swelling and shrinking of the polymer chain during the charging/discharging cycles. Tuning the side chains of conjugated polymers has profound impacts on morphology, crystallinity, charge carrier mobility, stability, and ion/water uptake properties. Attaching the optimal length of polar side chains, particularly OEG, on the polymers is a very promising technique to reduce the swelling and shrinking of the polymer electrodes and to enhance their suitability for SCs with aqueous electrolytes.[192] Furthermore, developing cross-linked polymers by incorporating cross-linkable side chains can also minimize the swelling and shrinking of the polymer electrodes by forming relatively stable film morphology.

6.3. Developing Stable n-Type Polymers

Developing stable n-type polymers in the negative potential regime is one of the challenges that limit the capacitance and potential window in the polymer-based SCs. One possible strategy to allow both facile diffusion and long-range charge delocalization is to develop n-type polymers by selecting complementary electroactive monomers and contorted aromatic

molecules.[42,193,194] D-A polymers consisting of strong acceptors and strong donors, which have redox-active groups, can be another strategy to develop efficient n-type polymer materials.

6.4. Enhancing the Potential Window

High potential window is crucial for achieving high energy density and cyclic stability. The incorporation of electron-withdrawing groups and 2D materials into the polymer backbone via covalent linkage can increase the potential window of the polymeric electrode materials. Assembling the materials in asymmetric SCs and employing organic electrolytes can further boost the potential windows and thereby energy densities of the devices. Preparation of D−node−A-type polymers, where acceptor and donor units are connected by a "node", could also be a promising strategy to develop ambipolar polymers with wider potential windows, high capacitance, and stability. Yet, the current knowledge of the D−n−A-type ambipolar polymers for SCs is limited and requires intensive research on their synthesis, characterization and optimization of the morphology.

The lack of standard device fabrication techniques and inconsistency in the calculation of energy density and power density are still hindering the development of SCs. In this regard, standard fabrication techniques for polymer-based SCs need to be developed in collaboration with engineers and industries to facilitate performance comparison and conversion into commercial products. Another barrier to the commercial application of polymer electrodes is severe capacitance loss with increased electrode thickness and mass loading as a result of slow mass transport (ion transport and electron transfer).[195] Thick electrodes create a considerable diffusion distance for electrolyte ions, reduce the accessible surface area, and are prone to significant cracking, leading to poor stability. Therefore, new strategies and in situ/*operando* techniques including in situ X-ray photoelectron spectroscopy (XPS), infrared/Fourier transform infrared spectroscopy (IR/FTIR), scanning electron microscopy (SEM), atomic force microscopy (AFM), scanning tunneling electron microscopy (STEM) and grazing incidence wide-angle X-ray scattering (GIWAXS) are required to study and address this issue.

With the increasing focus on performance enhancement and environmental sustainability in energy storage devices, there is a rising demand for electrode materials, manufacturing processes, and recycling methods that are both efficient and eco-friendly. In this context, biopolymer-based SCs emerge as a promising solution. Leveraging the abundance and cost-effectiveness of biopolymers like lignin and cellulose, the development of composite materials through in situ polymerization with conjugated polymers holds great potential. These advanced and biodegradable electrode materials can significantly enhance the efficiency and sustainability of SCs, paving the way for a greener future in energy storage.

From a synthesis point of view, green polymerization methods including direct arylation polycondensation, Buchwald/Hartwig coupling reactions, cross-dehydrogenative coupling (oxidative C–H/C–H coupling), and aldol condensation polymerization appear to be promising methods for the realization of high-performance and eco-friendly polymer-based SCs. However, further modifications are required to make these methods on par with the conventional methods for large-scale production of various polymers.

The unique advantages of polymer-based SCs, such as their electrochromic properties, flexibility, stretchability, long cycle lives, high reliability, and high power density, render them highly suitable and promising for various applications. Specifically, they hold great potential for integration into wearable, lightweight, and portable electronics. For instance, polymer-based SCs can be envisioned to power smart contact lenses that can be conveniently charged wirelessly. This exciting prospect exemplifies the potential impact of these advanced energy storage devices in transforming the landscape of electronic technologies.[196] Flexible and photorechargeable supercapacitors (SCs), which are all-solution-processable and made by integrating organic photovoltaics with SCs that share the same electrode, are emerging for their potential applications in smart electronics.[197] In this regard, considering the high processability and performance, as well as the dual function of polymers in solar cells and SCs, employing polymers as electrode materials in photo- rechargeable SCs, is a good strategy for achieving high-performance smart devices that may open a new era for SCs.

In view of the high energy density, power density, and excellent long-term cycling stability of polymer-based SCs and the rapid advancement of the design of the materials and the technology, conjugated polymers will be leading candidates for the commercialization of polymer-based SCs in the near future.

Acknowledgements

The authors thank The Swedish Energy Agency, The Swedish Research Council Formas, The Knut and Alice Wallenberg Foundation (2017.0186, 2022.0192), STINT (MG2021-9063), and the Wenner-Gren Foundations (UPD2021-0123) for financial support. W.M. further acknowledges the International Science Programme, Uppsala University, Sweden, for financial support.

Conflict of Interest

The authors declare no conflict of interest.

Keywords

conjugated polymers, cyclic voltammetry, electrolyte, pseudocapacitors, supercapacitors

Received: October 18, 2023
Revised: December 17, 2023
Published online:

[1] C. Schütter, S. Pohlmann, A. Balducci, *Adv. Energy Mater.* **2019**, *9*, 1900334.
[2] S. Fleischmann, J. B. Mitchell, R. Wang, C. Zhan, D. Jiang, V. Presser, V. Augustyn, *Chem. Rev.* **2020**, *120*, 6738.
[3] T. M. Gür, *Energy Environ. Sci.* **2018**, *11*, 2696.
[4] G. Zhou, F. Li, H.-M. Cheng, *Energy Environ. Sci.* **2014**, *7*, 1307.
[5] Y. Liang, C.-Z. Zhao, H. Yuan, Y. Chen, W. Zhang, J.-Q. Huang, D. Yu, Y. Liu, M.-M. Titirici, Y.-L. Chueh, H. Yu, Q. Zhang, *InfoMat* **2019**, *1*, 6.

[6] Y. Liu, Y. Zhu, Y. Cui, *Nat. Energy* **2019**, *4*, 540.
[7] B. Babu, P. Simon, A. Balducci, *Adv. Energy Mater.* **2020**, *10*, 2001128.
[8] B. Li, J. Zheng, H. Zhang, L. Jin, D. Yang, H. Lv, C. Shen, A. Shellikeri, Y. Zheng, R. Gong, J. P. Zheng, C. Zhang, *Adv. Mater.* **2018**, *30*, 1705670.
[9] A. Jagadale, X. Zhou, R. Xiong, D. P. Dubal, J. Xu, S. Yang, *Energy Storage Mater.* **2019**, *19*, 314.
[10] L. I. Schultz, N. P. Querques, *Renew. Sust. Energy Rev.* **2014**, *39*, 1119.
[11] F. Wang, X. Wu, X. Yuan, Z. Liu, Y. Zhang, L. Fu, Y. Zhu, Q. Zhou, Y. Wu, W. Huang, *Chem. Soc. Rev.* **2017**, *46*, 6816.
[12] N. R. Chodankar, H. D. Pham, A. K. Nanjundan, J. F. S. Fernando, K. Jayaramulu, D. Golberg, Y.-K. Han, D. P. Dubal, *Small* **2020**, *16*, 2002806.
[13] K. C. S. Lakshmi, X. Ji, T.-Y. Chen, B. Vedhanarayanan, T.-W. Lin, *J. Power Sources* **2021**, *511*, 230434.
[14] Y. Jiang, J. Liu, *Energy Environ. Mater.* **2019**, *2*, 30.
[15] T. Brousse, D. Bélanger, J. W. Long, *J. Electrochem. Soc.* **2015**, *162*, A5185.
[16] S. Balasubramaniam, A. Mohanty, S. K. Balasingam, S. J. Kim, A. Ramadoss, *Nano-Micro Lett.* **2020**, *12*, 85.
[17] X. Chen, R. Paul, L. Dai, *Natl. Sci. Rev.* **2017**, *4*, 453.
[18] M. Kaempgen, C. K. Chan, J. Ma, Y. Cui, G. Gruner, *Nano Lett.* **2009**, *9*, 1872.
[19] M. F. El-Kady, Y. Shao, R. B. Kaner, *Nat. Rev. Mater.* **2016**, *1*, 16033.
[20] J. Zhang, X. S. Zhao, *ChemSusChem* **2012**, *5*, 818.
[21] Z. Yu, L. Tetard, L. Zhai, J. Thomas, *Energy Environ. Sci.* **2015**, *8*, 702.
[22] V. Augustyn, P. Simon, B. Dunn, *Energy Environ. Sci.* **2014**, *7*, 1597.
[23] Q. Meng, K. Cai, Y. Chen, L. Chen, *Nano Energy* **2017**, *36*, 268.
[24] A. M. Bryan, L. M. Santino, Y. Lu, S. Acharya, J. M. D'Arcy, *Chem. Mater.* **2016**, *28*, 5989.
[25] T. Liu, L. Finn, M. Yu, H. Wang, T. Zhai, X. Lu, Y. Tong, Y. Li, *Nano Lett.* **2014**, *14*, 2522.
[26] S. Ghosh, T. Maiyalagan, R. N. Basu, *Nanoscale* **2016**, *8*, 6921.
[27] K. D. Fong, T. Wang, S. K. Smoukov, *Sustainable Energy Fuels* **2017**, *1*, 1857.
[28] L. Wang, Q. Wu, Z. Zhang, Y. Zhang, J. Pan, Y. Li, Y. Zhao, L. Zhang, X. Cheng, H. Peng, *J. Mater. Chem. A* **2016**, *4*, 3217.
[29] J. Kim, J. Lee, J. You, M.-S. Park, M. S. A. Hossain, Y. Yamauchi, J. H. Kim, *Mater. Horiz.* **2016**, *3*, 517.
[30] D. Dang, D. Yu, E. Wang, *Adv. Mater.* **2019**, *31*, 1970161.
[31] E. Wang, W. Mammo, M. R. Andersson, *Adv. Mater.* **2014**, *26*, 1801.
[32] T. Michinobu, *Chem. Soc. Rev.* **2011**, *40*, 2306.
[33] J. F. Mike, J. L. Lutkenhaus, *J. Polym. Sci., Part B: Polym. Phys.* **2013**, *51*, 468.
[34] M. E. Abdelhamid, A. P. O'Mullane, G. A. Snook, *RSC Adv.* **2015**, *5*, 11611.
[35] R. Chen, M. Yu, R. P. Sahu, I. K. Puri, I. Zhitomirsky, *Adv. Energy Mater.* **2020**, *10*, 1903848.
[36] Y. Han, L. Dai, *Macromol. Chem. Phys.* **2019**, *220*, 1800355.
[37] Z. Wang, M. Zhu, Z. Pei, Q. Xue, H. Li, Y. Huang, C. Zhi, *Mater. Sci. Eng. R Rep.* **2020**, *139*, 100520.
[38] G. Quek, B. Roehrich, Y. Su, L. Sepunaru, G. C. Bazan, *Adv. Mater.* **2021**, *34*, 2104206.
[39] H. Wu, Y. Zhang, W. Yuan, Y. Zhao, S. Luo, X. Yuan, L. Zheng, L. Cheng, *J. Mater. Chem. A* **2018**, *6*, 16617.
[40] A. Gupta, S. Sardana, J. Dalal, S. Lather, A. S. Maan, R. Tripathi, R. Punia, K. Singh, A. Ohlan, *ACS Appl. Energy Mater.* **2020**, *3*, 6434.
[41] R. Soni, V. Kashyap, D. Nagaraju, S. Kurungot, *ACS Appl. Mater. Interfaces* **2018**, *10*, 676.
[42] J. C. Russell, V. A. Posey, J. Gray, R. May, D. A. Reed, H. Zhang, L. E. Marbella, M. L. Steigerwald, Y. Yang, X. Roy, C. Nuckolls, S. R. Peurifoy, *Nat. Mater.* **2021**, *20*, 1136.
[43] C. Choi, D. S. Ashby, D. M. Butts, R. H. DeBlock, Q. Wei, J. Lau, B. Dunn, *Nat. Rev. Mater.* **2020**, *5*, 5.
[44] T. Pandolfo, V. Ruiz, S. Sivakkumar, J. Nerkar, in *Supercapacitors: Materials, Systems and Applications*, (Ed: F. Beguin, E. Frackowiak), WILEY-VCH, Weinheim, Germany **2013**, 87.
[45] N. Kurra, R. Wang, H. N. Alshareef, *J. Mater. Chem. A* **2015**, *3*, 7368.
[46] L. A. Estrada, D. Y. Liu, D. H. Salazar, A. L. Dyer, J. R. Reynolds, *Macromolecules* **2012**, *45*, 8211.
[47] A. Singh, A. Chandra, *Sci. Rep.* **2015**, *5*, 15551.
[48] Y. Shao, M. F. El-Kady, J. Sun, Y. Li, Q. Zhang, M. Zhu, H. Wang, B. Dunn, R. B. Kaner, *Chem. Rev.* **2018**, *118*, 9233.
[49] A. Noori, M. F. El-Kady, M. S. Rahmanifar, R. B. Kaner, M. F. Mousavi, *Chem. Soc. Rev.* **2019**, *48*, 1272.
[50] S. Zhang, N. Pan, *Adv. Energy Mater.* **2015**, *5*, 1401401.
[51] H. Shirakawa, E. J. Louis, A. G. MacDiarmid, C. K. Chiang, A. J. Heeger, *J. Chem. Soc., Chem. Commun.* **1977**, 578.
[52] Q. Fan, Q. An, Y. Lin, Y. Xia, Q. Li, M. Zhang, W. Su, W. Peng, C. Zhang, F. Liu, L. Hou, W. Zhu, D. Yu, M. Xiao, E. Moons, F. Zhang, T. D. Anthopoulos, O. Inganäs, E. Wang, *Energy Environ. Sci.* **2020**, *13*, 5017.
[53] Q. Fan, W. Su, S. Chen, T. Liu, W. Zhuang, R. Ma, X. Wen, Z. Yin, Z. Luo, X. Guo, L. Hou, K. Moth-Poulsen, Y. Li, Z. Zhang, C. Yang, D. Yu, H. Yan, M. Zhang, E. Wang, *Angew. Chem., Int. Ed.* **2020**, *59*, 19835.
[54] A. Minotto, P. Murto, Z. Genene, A. Zampetti, G. Carnicella, W. Mammo, M. R. Andersson, E. Wang, F. Cacialli, *Adv. Mater.* **2018**, *30*, 1706584.
[55] M. Kim, S. U. Ryu, S. A. Park, K. Choi, T. Kim, D. Chung, T. Park, *Adv. Funct. Mater.* **2020**, *30*, 1904545.
[56] M. Mone, S. Tang, Z. Genene, P. Murto, M. Jevric, X. Zou, J. Ràfols-Ribé, B. A. Abdulahi, J. Wang, W. Mammo, M. R. Andersson, L. Edman, E. Wang, *Adv. Optical Mater.* **2021**, *9*, 2001701.
[57] X. Liu, Y. Lin, Y. Liao, J. Wu, Y. Zheng, *J. Mater. Chem. C* **2018**, *6*, 3499.
[58] P. J. Nigrey, *J. Electrochem. Soc.* **1981**, *128*, 1651.
[59] M. G. Sumdani, M. R. Islam, A. N. A. Yahaya, S. I. Safie, *Polym. Eng. Sci.* **2022**, *62*, 269.
[60] G. A. Snook, P. Kao, A. S. Best, *J. Power Sources* **2011**, *196*, 1.
[61] M. Zhao, H. Zhang, C. Gu, Y. Ma, *J. Mater. Chem. C* **2020**, *8*, 5310.
[62] J. Heinze, B. A. Frontana-Uribe, S. Ludwigs, *Chem. Rev.* **2010**, *110*, 4724.
[63] K. Wang, J. Huang, Z. Wei, *J. Phys. Chem. C* **2010**, *114*, 8062.
[64] P. Novák, K. Müller, K. S. V. Santhanam, O. Haas, *Chem. Rev.* **1997**, *97*, 207.
[65] D. P. Dubal, S. H. Lee, J. G. Kim, W. B. Kim, C. D. Lokhande, *J. Mater. Chem.* **2012**, *22*, 3044.
[66] H. Li, J. Wang, Q. Chu, Z. Wang, F. Zhang, S. Wang, *J. Power Sources* **2009**, *190*, 578.
[67] Y. Huang, H. Li, Z. Wang, M. Zhu, Z. Pei, Q. Xue, Y. Huang, C. Zhi, *Nano Energy* **2016**, *22*, 422.
[68] R. B. Ambade, S. B. Ambade, N. K. Shrestha, Y.-C. Nah, S.-H. Han, W. Lee, S.-H. Lee, *Chem. Commun.* **2013**, *49*, 2308.
[69] A. M. Österholm, D. E. Shen, A. L. Dyer, J. R. Reynolds, *ACS Appl. Mater. Interfaces* **2013**, *5*, 13432.
[70] Y. Guo, W. Li, H. Yu, D. F. Perepichka, H. Meng, *Adv. Energy Mater.* **2017**, *7*, 1601623.
[71] G. P. Pandey, A. C. Rastogi, *Electrochim. Acta* **2013**, *87*, 158.
[72] D. Mo, W. Zhou, X. Ma, J. Xu, *Electrochim. Acta* **2015**, *155*, 29.
[73] W. Yao, P. Liu, C. Liu, J. Xu, K. Lin, H. Kang, M. Li, X. Lan, F. Jiang, *Chem. Eng. J.* **2022**, *428*, 131125.
[74] M. E. Roberts, D. R. Wheeler, B. B. McKenzie, B. C. Bunker, *J. Mater. Chem.* **2009**, *19*, 6977.
[75] Y. Zhang, F.-Q. Bai, Y. Xie, M. Zhu, L. Zhao, D. An, D. Xue, E. B. Berda, C. Wang, G. Lu, X. Jia, D. Chao, *Chem. Eng. J.* **2022**, *450*, 138386.
[76] D. Yiğit, M. Güllü, *J. Mater. Chem. A* **2017**, *5*, 609.

[77] A. Ringk, A. Lignie, Y. Hou, H. N. Alshareef, P. M. Beaujuge, *ACS Appl. Mater. Interfaces* **2016**, *8*, 12091.
[78] Z. Wang, X. Wang, S. Cong, F. Geng, Z. Zhao, *Mater. Sci. Eng. R Rep.* **2020**, *140*, 100524.
[79] P. Yang, P. Sun, Z. Chai, L. Huang, X. Cai, S. Tan, J. Song, W. Mai, *Angew. Chem., Int. Ed.* **2014**, *53*, 11935.
[80] G. Cai, P. Darmawan, M. Cui, J. Wang, J. Chen, S. Magdassi, P. S. Lee, *Adv. Energy Mater.* **2016**, *6*, 1501882.
[81] R. Yuksel, A. Ekber, J. Turan, E. Alpugan, S. O. Hacioglu, L. Toppare, A. Cirpan, G. Gunbas, H. E. Unalan, *Electroanalysis* **2018**, *30*, 266.
[82] Y. Kim, M. Han, J. Kim, E. Kim, *Energy Environ. Sci.* **2018**, *11*, 2124.
[83] G. Nie, L. Wang, C. Liu, *J. Mater. Chem. C* **2015**, *3*, 11318.
[84] X. Ma, W. Zhou, D. Mo, J. Hou, J. Xu, *Electrochim. Acta* **2015**, *176*, 1302.
[85] I. Marriam, Y. Wang, M. Tebyetekerwa, *Energy Storage Mater.* **2020**, *33*, 336.
[86] R. Wang, K. Lin, F. Jiang, W. Zhou, Z. Wang, Y. Wu, Y. Ding, J. Hou, G. Nie, J. Xu, X. Duan, *Electrochim. Acta* **2019**, *320*, 134641.
[87] Q. Guo, X. Zhao, Z. Li, B. Wang, D. Wang, G. Nie, *ACS Appl. Energy Mater.* **2020**, *3*, 2727.
[88] K. Bini, P. Murto, S. Elmas, M. R. Andersson, E. Wang, *Polym. Chem.* **2019**, *10*, 2004.
[89] S. Ming, K. Lin, H. Zhang, F. Jiang, P. Liu, J. Xu, G. Nie, X. Duan, *Chem. Commun.* **2020**, *56*, 5275.
[90] R. Wang, J. Li, L. Gao, J. Yu, *Chem. Eng. J.* **2022**, *445*, 136731.
[91] Y.-J. Hwang, T. Earmme, S. Subramaniyan, S. A. Jenekhe, *Chem. Commun.* **2014**, *50*, 10801.
[92] L. Xue, Y. Yang, J. Xu, C. Zhang, H. Bin, Z.-G. Zhang, B. Qiu, X. Li, C. Sun, L. Gao, J. Yao, X. Chen, Y. Yang, M. Xiao, Y. Li, *Adv. Mater.* **2017**, *29*, 1703344.
[93] H. Zhou, L. Yang, W. You, *Macromolecules* **2012**, *45*, 607.
[94] P. M. DiCarmine, T. B. Schon, T. M. McCormick, P. P. Klein, D. S. Seferos, *J. Phys. Chem. C* **2014**, *118*, 8295.
[95] W. Li, Y. Guo, Y. Wang, X. Xing, X. Chen, J. Ning, H. Yu, Y. Shi, I. Murtaza, H. Meng, *J. Mater. Chem. A* **2019**, *7*, 116.
[96] S. Ming, Z. Li, S. Zhen, P. Liu, F. Jiang, G. Nie, J. Xu, *Chem. Eng. J.* **2020**, *390*, 124572.
[97] H. Zhang, M. Yao, J. Wei, Y. Zhang, S. Zhang, Y. Gao, J. Li, P. Lu, B. Yang, Y. Ma, *Adv. Energy Mater.* **2017**, *7*, 1701063.
[98] L. Qin, W. Ma, M. Hanif, J. Jiang, Z. Xie, Y. Ma, *Macromolecules* **2017**, *50*, 3565.
[99] H. Wang, N. Jiang, Q. Zhang, G. Xie, N. Tang, L. Liu, Z. Xie, *Macromolecules* **2021**, *54*, 3469.
[100] M. B. Miltenburg, S. Y. An, N. K. Obhi, E. Grignon, B. T. McAllister, D. S. Seferos, *ACS Appl. Polym. Mater.* **2020**, *2*, 5574.
[101] J. Pu, Z. Shen, C. Zhong, Q. Zhou, J. Liu, J. Zhu, H. Zhang, *Adv. Mater.* **2020**, *32*, 1903808.
[102] J. Wu, Q. Zhang, J. Wang, X. Huang, H. Bai, *Energy Environ. Sci.* **2018**, *11*, 1280.
[103] R. Yuksel, S. C. Cevher, A. Cirpan, L. Toppare, H. E. Unalan, *J. Electrochem. Soc.* **2015**, *162*, A2805.
[104] A. M. Österholm, J. F. Ponder, J. A. Kerszulis, J. R. Reynolds, *ACS Appl. Mater. Interfaces* **2016**, *8*, 13492.
[105] A. M. Österholm, J. F. Ponder, M. De Keersmaecker, D. E. Shen, J. R. Reynolds, *Chem. Mater.* **2019**, *31*, 2971.
[106] L. R. Savagian, A. M. Österholm, J. F. Ponder Jr., K. J. Barth, J. Rivnay, J. R. Reynolds, *Adv. Mater.* **2018**, *30*, 1804647.
[107] M. Almtiri, T. J. Dowell, H. Giri, D. O. Wipf, C. N. Scott, *ACS Appl. Polym. Mater.* **2022**, *4*, 3088.
[108] Y. Sun, X. Zhao, G. Zhu, M. Li, X. Zhang, H. Yang, B. Lin, *Electrochim. Acta* **2020**, *333*, 135495.
[109] T. Ye, Y. Sun, X. Zhao, B. Lin, H. Yang, X. Zhang, L. Guo, *J. Mater. Chem. A* **2018**, *6*, 18994.
[110] T. Li, P. Liu, Y. Gao, S. Diao, X. Wang, B. Yang, X. Wang, *Mater. Lett.* **2019**, *244*, 13.
[111] T. Chu, X. Ju, X. Han, H. Du, Y. Zhang, J. Zhao, J. Zhang, *Org. Electron.* **2019**, *73*, 43.
[112] Y. Sun, G. Zhu, X. Zhao, W. Kang, M. Li, X. Zhang, H. Yang, L. Guo, B. Lin, *Sol. Energy Mater. Sol. Cells* **2020**, *215*, 110661.
[113] P. Murto, S. Elmas, U. A. Méndez-Romero, Y. Yin, Z. Genene, M. Mone, G. G. Andersson, M. R. Andersson, E. Wang, *Macromolecules* **2020**, *53*, 11106.
[114] J. F. Ponder, A. M. Österholm, J. R. Reynolds, *Chem. Mater.* **2017**, *29*, 4385.
[115] K. T. Sarang, A. Miranda, H. An, E.-S. Oh, R. Verduzco, J. L. Lutkenhaus, *ACS Appl. Polym. Mater.* **2019**, *1*, 1155.
[116] Y. Liang, Z. Chen, Y. Jing, Y. Rong, A. Facchetti, Y. Yao, *J. Am. Chem. Soc.* **2015**, *137*, 4956.
[117] Z. Genene, W. Mammo, E. Wang, M. R. Andersson, *Adv. Mater.* **2019**, *31*, 1807275.
[118] S. Sharma, R. Soni, S. Kurungot, S. K. Asha, *Macromolecules* **2018**, *51*, 954.
[119] S. Sharma, R. Soni, S. Kurungot, S. K. Asha, *J. Phys. Chem. C* **2019**, *123*, 2084.
[120] D. F. Zeigler, S. L. Candelaria, K. A. Mazzio, T. R. Martin, E. Uchaker, S.-L. Suraru, L. J. Kang, G. Cao, C. K. Luscombe, *Macromolecules* **2015**, *48*, 5196.
[121] K. Wang, L. Huang, N. Eedugurala, S. Zhang, M. A. Sabuj, N. Rai, X. Gu, J. D. Azoulay, T. N. Ng, *Adv. Energy Mater.* **2019**, *9*, 1902806.
[122] S. Wang, H. Sun, U. Ail, M. Vagin, P. O. Å. Persson, J. W. Andreasen, W. Thiel, M. Berggren, X. Crispin, D. Fazzi, S. Fabiano, *Adv. Mater.* **2016**, *28*, 10764.
[123] M. M. Alam, S. A. Jenekhe, *Chem. Mater.* **2004**, *16*, 4647.
[124] A. Babel, S. A. Jenekhe, *J. Am. Chem. Soc.* **2003**, *125*, 13656.
[125] A. V. Volkov, H. Sun, R. Kroon, T.-P. Ruoko, C. Che, J. Edberg, C. Müller, S. Fabiano, X. Crispin, *ACS Appl. Energy Mater.* **2019**, *2*, 5350.
[126] L. Jiao, Z. Hu, F. Ma, Y. He, Q. Zhou, L. Xiao, L. Lv, Y. Yang, *J. Energy Storage* **2022**, *52*, 104777.
[127] A. A. Szumska, I. P. Maria, L. Q. Flagg, A. Savva, J. Surgailis, B. D. Paulsen, D. Moia, X. Chen, S. Griggs, J. T. Mefford, R. B. Rashid, A. Marks, S. Inal, D. S. Ginger, A. Giovannitti, J. Nelson, *J. Am. Chem. Soc.* **2021**, *143*, 14795.
[128] S. T. M. Tan, T. J. Quill, M. Moser, G. LeCroy, X. Chen, Y. Wu, C. J. Takacs, A. Salleo, A. Giovannitti, *ACS Energy Lett.* **2021**, *6*, 3450.
[129] D. Moia, A. Giovannitti, A. A. Szumska, I. P. Maria, E. Rezasoltani, M. Sachs, M. Schnurr, P. R. F. Barnes, I. McCulloch, J. Nelson, *Energy Environ. Sci.* **2019**, *12*, 1349.
[130] R. M. Pankow, B. C. Thompson, *Polym. Chem.* **2020**, *11*, 630.
[131] J. Xie, C. Zhao, Z. Lin, P. Gu, Q. Zhang, *Chem. Asian J.* **2016**, *11*, 1489.
[132] J. Jiang, Y. Zhang, P. Nie, G. Xu, M. Shi, J. Wang, Y. Wu, R. Fu, H. Dou, X. Zhang, *Adv. Sustainable Syst.* **2018**, *2*, 1700110.
[133] J. R. Potts, D. R. Dreyer, C. W. Bielawski, R. S. Ruoff, *Polymer* **2011**, *52*, 5.
[134] A. Sajedi-Moghaddam, C. C. Mayorga-Martinez, Z. Sofer, D. Bouša, E. Saievar-Iranizad, M. Pumera, *J. Phys. Chem. C* **2017**, *121*, 20532.
[135] L. Wang, X. Lu, S. Lei, Y. Song, *J. Mater. Chem. A* **2014**, *2*, 4491.
[136] V. Vijayakumar, B. Anothumakkool, S. Kurungot, M. Winter, J. R. Nair, *Energy Environ. Sci.* **2021**, *14*, 2708.
[137] W. Tian, X. Mao, P. Brown, G. C. Rutledge, T. A. Hatton, *Adv. Funct. Mater.* **2015**, *25*, 4803.
[138] H.-P. Cong, X.-C. Ren, P. Wang, S.-H. Yu, *Energy Environ. Sci.* **2013**, *6*, 1185.
[139] J. Wu, Q. Zhang, A. Zhou, Z. Huang, H. Bai, L. Li, *Adv. Mater.* **2016**, *28*, 10211.
[140] J. Zhu, W. Sun, D. Yang, Y. Zhang, H. H. Hoon, H. Zhang, Q. Yan, *Small* **2015**, *11*, 4123.

[141] D. D. Potphode, L. Sinha, P. M. Shirage, *Appl. Surf. Sci.* **2019**, *469*, 162.
[142] K. Wang, L. Li, Y. Liu, C. Zhang, T. Liu, *Adv. Mater. Interfaces* **2016**, *3*, 1600665.
[143] S. Kulandaivalu, Y. Sulaiman, *J. Power Sources* **2019**, *419*, 181.
[144] Y. Li, M. Zhou, Y. Wang, Q. Pan, Q. Gong, Z. Xia, Y. Li, *Carbon* **2019**, *147*, 519.
[145] M. Zhou, Y. Li, Q. Gong, Z. Xia, Y. Yang, X. Liu, J. Wang, Q. Gao, *ChemElectroChem* **2019**, *6*, 4595.
[146] N. An, Z. Shao, Z. Guo, J. Xin, Y. He, L. Lv, K. Xie, X. Dong, Y. Zhang, Z. Hu, *J. Power Sources* **2020**, *475*, 228692.
[147] B. A. Wavhal, M. Ghosh, S. Sharma, S. Kurungot, A. Sk, *Nanoscale* **2021**, *13*, 12314.
[148] Z.-J. Cai, Q. Zhang, X.-Y. Song, *Electron. Mater. Lett.* **2016**, *12*, 830.
[149] M. Sun, G. Wang, C. Yang, H. Jiang, C. Li, *J. Mater. Chem. A* **2015**, *3*, 3880.
[150] L. Qin, Q. Tao, A. El Ghazaly, J. Fernandez-Rodriguez, P. O. Å. Persson, J. Rosen, F. Zhang, *Adv. Funct. Mater.* **2018**, *28*, 1703808.
[151] S. Panda, K. Deshmukh, S. K. Khadheer Pasha, J. Theerthagiri, S. Manickam, M. Y. Choi, *Coord. Chem. Rev.* **2022**, *462*, 214518.
[152] M. Boota, B. Anasori, C. Voigt, M.-Q. Zhao, M. W. Barsoum, Y. Gogotsi, *Adv. Mater.* **2016**, *28*, 1517.
[153] W. Zhang, J. Ma, W. Zhang, P. Zhang, W. He, J. Chen, Z. Sun, *Nanoscale* **2020**, *12*, 6637.
[154] X. Li, J. Hao, R. Liu, H. He, Y. Wang, G. Liang, Y. Liu, G. Yuan, Z. Guo, *Energy Storage Mater.* **2020**, *33*, 62.
[155] A. VahidMohammadi, J. Moncada, H. Chen, E. Kayali, J. Orangi, C. A. Carrero, M. Beidaghi, *J. Mater. Chem. A* **2018**, *6*, 22123.
[156] S. De, C. K. Maity, S. Sahoo, G. C. Nayak, *ACS Appl. Energy Mater.* **2021**, *4*, 3712.
[157] Z. Sun, K. Qu, Y. You, Z. Huang, S. Liu, J. Li, Q. Hu, Z. Guo, *J. Mater. Chem. A* **2021**, *9*, 7278.
[158] S. Li, D. Huang, B. Zhang, X. Xu, M. Wang, G. Yang, Y. Shen, *Adv. Energy Mater.* **2014**, *4*, 1301655.
[159] G. Z. Chen, *Prog. Nat. Sci. Mater. Int.* **2021**, *31*, 792.
[160] Y. Liu, J. Zhou, J. Tang, W. Tang, *Chem. Mater.* **2015**, *27*, 7034.
[161] N. A. A. Sezali, H. L. Ong, N. Jullok, A. R. Villagracia, R.-A. Doong, *Macromol. Mater. Eng.* **2021**, *306*, 2100556.
[162] Y. Chen, S. Lyu, S. Han, Z. Chen, W. Wang, S. Wang, *RSC Adv.* **2018**, *8*, 39918.
[163] S. Admassie, A. Elfwing, E. W. H. Jager, Q. Bao, O. Inganäs, *J. Mater. Chem. A* **2014**, *2*, 1974.
[164] D. H. Nagaraju, T. Rebis, R. Gabrielsson, A. Elfwing, G. Milczarek, O. Inganäs, *Adv. Energy Mater.* **2014**, *4*, 1300443.
[165] G. Milczarek, O. Inganäs, *Science* **2012**, *335*, 1468.
[166] H. Wang, F. Li, B. Zhu, L. Guo, Y. Yang, R. Hao, H. Wang, Y. Liu, W. Wang, X. Guo, X. Chen, *Adv. Funct. Mater.* **2016**, *26*, 3472.
[167] A. Mukhopadhyay, Y. Jiao, R. Katahira, P. N. Ciesielski, M. Himmel, H. Zhu, *Nano Lett.* **2017**, *17*, 7897.
[168] G. Hernández, N. Casado, A. M. Zamarayeva, J. K. Duey, M. Armand, A. C. Arias, D. Mecerreyes, *ACS Appl. Energy Mater.* **2018**, *1*, 7199.
[169] S. Admassie, F. N. Ajjan, A. Elfwing, O. Inganäs, *Mater. Horiz.* **2016**, *3*, 174.
[170] S. Chaleawlert-umpon, T. Berthold, X. Wang, M. Antonietti, C. Liedel, *Adv. Mater. Interfaces* **2017**, *4*, 1700698.
[171] F. N. Ajjan, N. Casado, T. Rębiś, A. Elfwing, N. Solin, D. Mecerreyes, O. Inganäs, *J. Mater. Chem. A* **2016**, *4*, 1838.
[172] J. Edberg, O. Inganäs, I. Engquist, M. Berggren, *J. Mater. Chem. A* **2018**, *6*, 145.
[173] D. Wu, W. Zhong, *J. Mater. Chem. A* **2019**, *7*, 5819.
[174] C. Beaumont, S. Naqvi, M. Leclerc, *Trends Chem* **2022**, *4*, 714.
[175] B. Pal, S. Yang, S. Ramesh, V. Thangadurai, R. Jose, *Nanoscale Adv* **2019**, *1*, 3807.
[176] L. Sun, K. Zhuo, Y. Chen, Q. Du, S. Zhang, J. Wang, *Adv. Funct. Mater.* **2022**, *32*, 2203611.
[177] C. Zhong, Y. Deng, W. Hu, J. Qiao, L. Zhang, J. Zhang, *Chem. Soc. Rev.* **2015**, *44*, 7484.
[178] L. Kou, T. Huang, B. Zheng, Y. Han, X. Zhao, K. Gopalsamy, H. Sun, C. Gao, *Nat. Commun.* **2014**, *5*, 3754.
[179] L. Yuan, B. Yao, B. Hu, K. Huo, W. Chen, J. Zhou, *Energy Environ. Sci.* **2013**, *6*, 470.
[180] Y. Huang, J. Tao, W. Meng, M. Zhu, Y. Huang, Y. Fu, Y. Gao, C. Zhi, *Nano Energy* **2015**, *11*, 518.
[181] D. Vonlanthen, P. Lazarev, K. A. See, F. Wudl, A. J. Heeger, *Adv. Mater.* **2014**, *26*, 5095.
[182] W. Zhao, Y. Li, S. Wu, D. Wang, X. Zhao, F. Xu, M. Zou, H. Zhang, X. He, A. Cao, *ACS Appl. Mater. Interfaces* **2016**, *8*, 34027.
[183] W. Zhao, S. Wang, C. Wang, S. Wu, W. Xu, M. Zou, A. Ouyang, A. Cao, Y. Li, *Nanoscale* **2016**, *8*, 626.
[184] K. Li, J. Liu, Y. Huang, F. Bu, Y. Xu, *J. Mater. Chem. A* **2017**, *5*, 5466.
[185] G.-P. Hao, F. Hippauf, M. Oschatz, F. M. Wisser, A. Leifert, W. Nickel, N. Mohamed-Noriega, Z. Zheng, S. Kaskel, *ACS Nano* **2014**, *8*, 7138.
[186] Y. Huang, M. Zhu, Z. Pei, Y. Huang, H. Geng, C. Zhi, *ACS Appl. Mater. Interfaces* **2016**, *8*, 2435.
[187] J. D. Stenger-Smith, C. K. Webber, N. Anderson, A. P. Chafin, K. Zong, J. R. Reynolds, *J. Electrochem. Soc.* **2002**, *149*, A973.
[188] D. Y. Liu, J. R. Reynolds, *ACS Appl. Mater. Interfaces* **2010**, *2*, 3586.
[189] H. Zhang, X. Tang, D. Zhao, N. Zheng, L. Huang, T. Sun, C. Gu, Y. Ma, *Energy Storage Mater.* **2020**, *29*, 281.
[190] T. Liu, Y. Li, *InfoMat* **2020**, *2*, 807.
[191] M. Kim, C. Lee, J. Jang, *Adv. Funct. Mater.* **2014**, *24*, 2489.
[192] J. W. Onorato, Z. Wang, Y. Sun, C. Nowak, L. Q. Flagg, R. Li, B. X. Dong, L. J. Richter, F. A. Escobedo, P. F. Nealey, S. N. Patel, C. K. Luscombe, *J. Mater. Chem. A* **2021**, *9*, 21410.
[193] S. R. Peurifoy, J. C. Russell, T. J. Sisto, Y. Yang, X. Roy, C. Nuckolls, *J. Am. Chem. Soc.* **2018**, *140*, 10960.
[194] C. Schaack, A. M. Evans, F. Ng, M. L. Steigerwald, C. Nuckolls, *J. Am. Chem. Soc.* **2021**, *144*, 42.
[195] W. Guo, C. Yu, S. Li, J. Qiu, *Energy Environ. Sci.* **2021**, *14*, 576.
[196] J. Park, D. B. Ahn, J. Kim, E. Cha, B. S. Bae, S.-Y. Lee, J.-U. Park, *Sci. Adv.* **2019**, *5*, eaay0764.
[197] N. K., C. S. Rout, *J. Mater. Chem. A* **2021**, *9*, 8248.

Zewdneh Genene received his PhD in organic chemistry from the Department of Chemistry, Addis Ababa University, Ethiopia in 2017. He was a visiting PhD student at the Department of Chemistry and Chemical Engineering, Chalmers University of Technology, Sweden (2015–2016). From 2017–2021, he served as an assistant professor at the Department of Chemistry, Ambo University, Ethiopia. From 2019 to 2023, he worked as postdoctoral researcher at Chalmers University of Technology, Sweden. His research focuses on the design, synthesis, and characterization of conjugated polymers and small molecules for applications in organic solar cells, light-emitting electrochemical cells, supercapacitors, and photocatalytic hydrogen production.

Ergang Wang is a Professor in the Department of Chemistry and Chemical Engineering at Chalmers University of Technology. He previously served as a postdoctoral fellow in the same department from 2008 to 2011. He earned his PhD in Materials Science from the South China University of Technology in 2008. His research is primarily focused on advancing the field of conjugated polymers and 2D materials. His work spans a range of applications including organic solar cells, photodetectors, light-emitting electrochemical cells, field-effect transistors, supercapacitors, and photocatalytic hydrogen evolution reactions.